# UNITED STATES
# DEPARTMENT OF THE INTERIOR
# U.S. GEOLOGICAL SURVEY

---

## ESTIMATION OF RESPONSE SPECTRA AND PEAK ACCELERATIONS FROM WESTERN NORTH AMERICAN EARTHQUAKES: AN INTERIM REPORT

### PART 2

David M. Boore, William B. Joyner, and Thomas E. Fumal

---

# INTRODUCTION

More than a decade ago we presented equations for predicting peak horizontal acceleration and response spectra in terms of moment magnitude, distance, and site conditions for shallow earthquakes in western North America (Joyner and Boore, 1981, 1982). We are currently developing a new set of equations taking account of the data recorded since 1980. In addition to incorporating the new data, we plan to reprocess all the data for greater uniformity and for the purpose of extending the period range to as long a period as possible. Because of the time that will be required to complete the long-term project, we decided to present an interim report (Boore *et al.*, 1993, hereafter referred to as "BJF93") updating our earlier equations to incorporate data from three recent California earthquakes (Loma Prieta, 1989, Petrolia, 1992, and Landers, 1992) that provided data in the large-magnitude, close-distance range where the earlier data set was severely deficient. In addition to including the new data, we changed the site classification system to a three-category classification based on average shear-wave velocity to a depth of 30 m. Other changes are described in BJF93. In order to make the new equations available as soon as possible, we published the interim report before we had completed several auxiliary studies of the data set. Those additional studies are the subject of this report, which we designate as part two of the interim report.

This report contains ten items, summarized below. In general, new topics not contained in BJF93 are discussed first.

1. As an alternative to the three-category site classification, we present a way of calculating the site effect as a continuous function of the average shear-wave velocity to a depth of 30 m.

2. We study residuals within 10 km and perform a Monte Carlo simulation study to see if the scaling with magnitude at close distances is different from that at larger distances.

3. We examine residuals for the BJF93 equations to see if the variance depends on magnitude or if it depends on ground-motion amplitude.

4. We examine differences in ground motion between strike-slip and reverse-slip earthquakes.

5. We perform a Monte Carlo simulation study to assess the sensitivity of the predicted values to stochastic uncertainties in the regression coefficients.

6. We compare response spectra predicted from equations developed by one-stage and two-stage maximum-likelihood methods.

7. We present plots showing how residuals for peak horizontal acceleration depend on magnitude, distance, and site conditions (similar plots were given in BJF93 for response spectra but not for peak acceleration).

8. We include equations for predicting smoothed response spectra in terms of cubic polynomials in period, from which predictions can be obtained for periods not included in BJF93.

9. We discuss limitations of the present equations and prospects for improvement in future work.

10. We include errata for BJF93.

The one-stage and two-stage calculations in this report and in BJF93 were done by the methods described by Joyner and Boore (1993) as corrected (Joyner and Boore, 1994), except that, in the first stage of the two-stage regression, the sum of square errors was minimized with respect to the parameter $h$ in equation (2) of BJF93 by a simple numerical search (using the routine GOLDEN [Press *et al.*, 1992]) rather than by linearization as described in Joyner and Boore (1993).

## THE SITE EFFECT IN TERMS OF SHEAR-WAVE VELOCITY

In the equations of BJF93 the site-effect term takes on different values depending on whether the average shear-wave velocity to a depth of 30 m is greater than 750 m/s (Class A), between 360 and 750 m/s (Class B), or between 180 and 360 m/s (Class C). The class definitions are taken from site-effects provisions proposed for the 1994 National Earthquake Hazards Reduction Program (NEHRP) model building-code provisions. (The NEHRP proposal also has a Class D with average velocity less than 180 m/s, but Class D was poorly represented in the BJF93 data set and was excluded from the analysis.) We are confident that the use of a classification system based entirely on shear-wave velocity represents an improvement over systems based on subjective descriptions of site geology. Even though the classification system is an improvement, it would be better still to compute

3

the site effect as a continuous function of shear-wave velocity, if available. We have done that, generally following the ideas of Joyner and Fumal (1984).

For more than half the records used in developing the BJF93 equations the time-weighted average shear-wave velocities to 30 m ($V_S$) have been obtained from downhole surveys at the sites (a histogram of these velocities is shown in Figure 1, and the recordings used in the analysis are listed in Table 1). The average is computed by dividing 30 m by the S-wave travel time to 30 m (in contrast to a depth-weighted average found by dividing the sum of the product of the layer thickness and velocity by 30 m). For those records, we take the residuals ($R$) with respect to the BJF93 equations for site Class A and fit the following functional form to the residuals by two-stage regression:

$$\log R = b_V(\log V_S - \log V_A) + \epsilon_r + \epsilon_e. \tag{1}$$

In this equation $\log R$ is the residual (log observed minus log predicted ground motion), $\epsilon_r$ is an independent random variable that takes on a specific value for each record, and $\epsilon_e$ is an independent random variable that takes on a specific value for each earthquake. The coefficients to be determined are $b_V$ and $\log V_A$. In the first stage of the two-stage regression the coefficient $b_V$ is determined along with a set of amplitude factors, one for each earthquake. In the second stage a weighted average of the amplitude factors gives the product$(-b_V \log V_A)$ from which $V_A$ is obtained. The weight $w_i$ for each earthquake is given by

$$w_i = (\sigma_1^2/N_{r_i} + \sigma_e^2)^{-1}, \tag{2}$$

where $\sigma_1^2$ is the variance of the first stage, $N_{r_i}$ is number of recordings for earthquake $i$, and $\sigma_e^2$ is the intrinsic variance of the amplitude factors. The value of $\sigma_e^2$ was determined by requiring that the weighted sum of square deviations of the amplitude factors from the mean be equal (or as close as possible to) the number of degrees of freedom, $N_e - 1$, where $N_e$ is the number of earthquakes. To show graphically the amplification as a function of velocity, we removed the earthquake-to-earthquake variation by subtracting from the residuals a constant given by evaluating, at a velocity equal to $V_A$, the straight-line fit determined for each earthquake in the first stage of the regression. Figure 2 shows the results for 5 percent damping and a set of eight oscillator periods uniformly distributed logarithmically between 0.1 and 2 seconds (we use this set of periods for many of the graphical results shown in this report). The plots show strong correlation of long-period ground motion with shear-wave velocity. The values of $b_V$ and $\log V_A$ are smoothed by least-squares fitting of a cubic polynomial as was done for the coefficients of the BJF93

4

equations. The results are given in Table 2 for response spectra and Table 3 for peak acceleration. The term

$$b_V(\log V_S - \log V_A) \qquad (3)$$

replaces the term

$$b_6 G_B + b_7 G_C$$

in equation (1) of BJF93. The effect on the variance is negligible, and the standard deviation values from Tables 7, 8, and 9 of BJF93 should be used for these computations as well. (The equations in BJF93 give pseudo-velocity response spectra ($psv$); acceleration spectra ($S_A$), defined as $(2\pi/T)psv$, can be obtained by adding the column labeled "BSA" in Table 2 to equation (1) in BJF93, where the units of $S_A$ are the acceleration of gravity ($g$).)

The dependence of the amplification on shear velocity is given by the coefficient $b_V$ in equation (3). As shown in Figure 3, the velocity dependence is remarkably similar to that determined by Midorikawa (written comm., 1993) in Japan and to the coefficients proposed by Borcherdt (1994) for use in determining short- and mid-period amplification factors in building codes.

## MAGNITUDE SCALING AT SHORT DISTANCES

Equations given by many authors for predicting ground-motion values have smaller magnitude scaling at short distances than at long distances (*e.g.* Campbell and Bozorgnia, 1994). Our equations have the same magnitude scaling at all distances. Until recently there were no data available to constrain the equations for large earthquakes at close distances, and under these circumstances the differences in magnitude scaling could lead to substantial differences in the predicted ground motions. The 1989 Loma Prieta, 1992 Petrolia, and 1993 Landers earthquakes have provided data in the critical large-magnitude, close-distance range, however, limiting the variations in predicted motions permitted by the data. To see if our data set would support a smaller magnitude scaling at short distance, we took residuals at stations within 10 km with respect to the equation determined for the whole data set. We then used the two-stage regression method to find the linear function of magnitude that best fit the residuals. The results are shown in Figure 4 for peak horizontal acceleration and response spectra at 5 percent damping and 8 periods from 0.1 to 2.0 sec. The slopes of the best-fitting straight lines are positive in some cases and negative in others. The absolute value of the slope is less than the standard error of the slope for peak acceleration and for response spectra at all but one of the 8 periods (0.85

5

sec). We conclude there is no support in the data for smaller magnitude scaling at short distance.

We also used Monte Carlo simulation (Press *et al.*, 1992) to examine the question of magnitude scaling at close distance. A different magnitude scaling at close distance can be obtained by setting the parameter $h$ in equation (2) of BJF93 equal to

$$h_1 \exp(h_2[\mathbf{M} - 6]). \tag{4}$$

We take as our null hypothesis that $h_2 = 0$ and see if that hypothesis is compatible with the data. To do so we start with an input set of parameter values determined by fitting the real data set with $h_2$ constrained to be zero. We take the magnitude, distance, and site-condition values from the data set and use the input parameter set in equation (1) of BJF93 with the aid of a pseudorandom-number generator to simulate a set of ground-motion values, which we analyze by the two-stage method with $h$ given by equation (4). We do 100 simulations for peak horizontal acceleration and 100 simulations for response spectra at 5 percent damping and each of 8 periods equally spaced logarithmically between 0.1 and 2.0 sec. We then analyze the real data using the two-stage method with $h$ given by equation (4). (In the first stage the sum of square errors is minimized with respect to $h_1$ and $h_2$ by the downhill simplex method [Press *et al.*, 1992].) The $h_2$ values determined from the real data are compared in Figure 5 with the distribution of values simulated under the null hypothesis. For peak acceleration the value determined from the data is at the 31st percentile level of the distribution of simulated values. For the response spectra, the smallest value is at the 6th percentile level, two values are smaller than the 10th percentile level, and the remaining six are less than the 90th percentile level. We see no basis for rejecting the null hypothesis $h_2 = 0$.

## THE EFFECT OF MAGNITUDE AND AMPLITUDE ON VARIANCE

*Dependence on Magnitude.* A number of authors have suggested that the variance of peak horizontal acceleration depends on magnitude (for example, Idriss, 1985, and Youngs *et al.*, 1994, who show that the dependence is statistically significant). We examine the suggestion for our data, using prediction equations derived by the one-stage maximum-likelihood method to make the results comparable to those of Youngs *et al.* (1994). We divide the data into three magnitude classes, 5.00–5.99, 6.00–6.99, and 7.00–7.99, and take the residuals in each class with respect to the equation determined for the whole data set. For each class we determine the variance $\sigma_c^2$ of the horizontal components (BJF93, equation [3]). Then for

6

each class we average the residuals of the two horizontal components and use the one-stage maximum-likelihood method to determine $\sigma_e^2$, the earthquake-to earthquake component of the variance, and $\sigma_1^2$, which represents the remaining components of variability. The total variance $\sigma_{\log Y}^2$ is equal to $\sigma_1^2 + \sigma_e^2 + \sigma_c^2$. To estimate the standard error of the total variance we use the large-sample expressions given by Searle (1971, p.474) for the variance of $\sigma_1^2$ and $\sigma_e^2$ and the covariance of $\sigma_1^2$ and $\sigma_e^2$, and we assume that $\sigma_c^2$ is independent of $\sigma_1^2$ and $\sigma_e^2$, an assumption that may not be strictly correct. The results for peak horizontal acceleration and response spectral values at eight periods are given in Figure 6, which shows the estimate of $\sigma_{\log Y}$ for each magnitude class with error bars corresponding to plus and minus one standard error of $\sigma_{\log Y}^2$. For peak acceleration we, like Youngs *et al.* (1994), find that $\sigma_{\log Y}$ decreases with increasing magnitude and we, like they, find that most of the effect appears below magnitude 6.0. For response spectral values we see no significant dependence of variance on magnitude. The difference between the results for peak acceleration and response spectral values is probably due, at least in part, to the relatively few records in the response spectral data set from earthquakes with magnitude less than 6.0 (1 and 5 records from earthquakes of magnitude 5.3 and 5.8, respectively; see Figure 1 in BJF93).

*Dependence on Amplitude.* Some authors have suggested that the variance of peak horizontal acceleration depends on the value of peak acceleration (Donovan and Bornstein, 1978; Campbell and Bozorgnia, 1994). We examine our peak acceleration data for such dependence using equation (1) in BJF93. We divide the data into three classes, using a three-to-one ratio between the values defining the middle class: 1) those records for which the predicted peak acceleration is less than 0.1 $g$, 2) those for which the predicted value falls between 0.1 and 0.3 $g$, and 3) those for which the predicted value is greater than or equal to 0.3 $g$. As above we determine, for each class, the variance $\sigma_c^2$ of the horizontal components (BJF93, equation [3]). Then, for each class, we average the residuals of the two horizontal components and use the one-stage maximum-likelihood method to determine $\sigma_e^2$, the earthquake-to earthquake component of the variance, and $\sigma_1^2$ which represents the remaining components of variability. We also study the response-spectral data for evidence of an amplitude-dependent variance. As before, we maintain a three-to-one ratio between the boundary values used to define the middle amplitude class and adjust the values to maintain a sufficient number of data points in each category. The boundary values, which depend on oscillator period, are given in Table 4. The values of $\sigma_{\log Y}^2$ for each class are determined as described above. The results for peak horizontal acceleration and response spectral values at eight periods are given in Figure 7, which shows the estimate of $\sigma_{\log Y}$ for

each amplitude class with error bars corresponding to plus and minus one standard error of $\sigma^2_{\log Y}$. For peak acceleration we, like Campbell and Bozorgnia (1994), find that $\sigma_{\log Y}$ decreases with increasing peak acceleration. Figure 7 shows that most of the effect for peak acceleration with our data set appears for Amplitude Class 1 (below 0.1 $g$). For response spectra our data set shows no clear trend. The difference between peak acceleration and response spectra reflects in part the relatively fewer low-amplitude data points in the response spectral data set.

## THE EFFECT OF FOCAL MECHANISM ON RESPONSE SPECTRAL VALUES

Many authors (most recently Campbell and Bozorgnia, 1994) have proposed that ground-motion values depend on the focal mechanism of the earthquake. We examine that proposition for response spectra. Table 5 gives the rake angles for the earthquakes in the response spectral data set, using the convention of Aki and Richards (1980) that reverse slip earthquakes have positive rake angles, and the absolute value of the rake for left-lateral slip is less than 90 degrees. The rake angle for the Daly City earthquake is indeterminate (given by 999 in Table 5), because the fault plane is indistinguishable from horizontal. We define strike-slip earthquakes as those with a rake angle within 30 degrees of horizontal. The remaining earthquakes are reverse-slip, because there are no normal-slip events in the data set. We do a two-stage regression analysis using equation [1] in BJF93, except in the second stage we replace the constant term $b_1$ by $b_{SS}G_{SS} + b_{RS}G_{RS}$, where $G_{SS} = 1$ for a strike-slip earthquake and zero otherwise, $G_{RS} = 1$ for a reverse-slip earthquake and zero otherwise, and $b_{SS}$ and $b_{RS}$ are coefficients to be determined. The magnitude-dependence given by coefficients $b_2$ and $b_3$ values need not be the same as before. In fact, for all periods the quadratic magnitude dependence ($b_3$) is small compared to the uncertainty in the coefficient. For this reason, we reran the problem constraining $b_3$ to be zero. The ratio of the response spectral values between reverse- and strike-slip earthquakes ($Y_{RS}/Y_{SS}$) is given by 10 raised to the power $b_{RS} - b_{SS}$. This ratio is plotted against period in Figure 8. The error bars represent plus and minus one standard deviation of the difference. The plotted values can be thought of as the difference in the logarithm of Figure 8 shows that the response spectral values are larger for reverse-slip earthquakes than for strike-slip earthquakes, but the differences are relatively small and of marginal significance statistically. We await our future analysis using the more complete data set before deciding whether or not focal mechanism should be used as a predictor variable.

## SENSITIVITY OF PREDICTION ERROR TO PARAMETER UNCERTAINTY

We used Monte Carlo simulation (Press *et al.*, 1992) to evaluate the contribution to prediction error from stochastic uncertainty in the parameters of the prediction equations. We start with an input set of parameter values determined by fitting the real data set. We take the magnitude, distance, and site-condition values from the data set and use the input parameter set in equation (1) of BJF93 with the aid of a pseudorandom-number generator to simulate a set of ground-motion values, which we analyze by the two-stage method to obtain a set of simulated parameters. We then use the set of simulated parameters to predict ground-motion values at Class C sites for $\mathbf{M} = 6.5$ and 7.5 at $d = 0$ and 20 km. We used 100 simulations for peak horizontal acceleration and 100 simulations for response spectra at 5 percent damping and each of 8 periods from 0.1 to 2.0 sec. The mean predicted values of the ground motions from the simulations are within about 3% of the ground-motion values predicted from the input parameters. This close agreement indicates that there is no bias introduced by the particular distribution of the data set over magnitude, distance, and site condition and no bias introduced by the analysis method. The contribution to prediction error from stochastic uncertainties in the parameters is less than 35 percent for $d = 0$ km and substantially less at $d = 20$ km. These contributions are small compared to the standard error of an individual prediction.

## RESIDUALS OF PEAK HORIZONTAL ACCELERATION

Figure 9 gives the average residual for the two horizontal components of peak acceleration plotted against distance for different site and magnitude classes for the prediction equations of BJF93. Similar plots were presented in BJF93 for response spectra at 0.3 s and 1.0 s and 5-percent damping.

## PREDICTION EQUATIONS AS CONTINUOUS FUNCTIONS OF PERIOD

Even though we evaluated the regression coefficients at a relatively dense set of oscillator periods, for some purposes it may be desired to predict response spectra at other periods. A convenient way to do this is to take advantage of our smoothing of the coefficients over period. As discussed in BJF93, we settled on fitting the regression coefficients by cubic polynomials in $\log T$ as follows:

$$B = C_0 + C_1 \log T + C_2 (\log T)^2 + C_3 (\log T)^3, \tag{5}$$

9

where $B$ is a regression coefficient. We give the polynomial coefficients for the prediction of response spectra in terms of site classes in Tables 6 and 7 and in terms of average-shear wave velocity in Tables 8 and 9. These coefficients should *not* be used to predict response spectra outside of the period range from 0.1 to 2.0 sec (where the coefficients were determined). Extension of the cubic polynomial outside that range is likely to lead to ridiculous results.

## COMPARISON OF ONE-STAGE AND TWO-STAGE MAXIMUM-LIKELIHOOD METHODS

The equations for response spectra given in BJF93 were obtained with the two-stage maximum-likelihood method. One-stage maximum-likelihood methods have been proposed (for example, Brillinger and Preisler, 1984, 1985), and we here compare spectra obtained using one-stage and two-stage methods (for the one-stage method we used the procedure described in Joyner and Boore, 1993). The results were very similar as illustrated by Figure 10, which compares unsmoothed, five-percent-damped spectra for the random horizontal component computed using the one-stage method (heavy lines) with spectra computed using the two-stage method (light lines) for a C site in a magnitude 7.5 earthquake at distances of 0, 10, 20, 40, and 80 km.

## LIMITATIONS OF THE PRESENT WORK AND PROSPECTS FOR IMPROVEMENT

*Few response spectral data below magnitude 6.0.* Earthquakes with magnitudes less than 6.0 are poorly represented in the response-spectral data set, which includes only one record from a magnitude 5.3 earthquake and six records from a magnitude 5.8 earthquake. Prediction of ground motion for the smaller earthquakes is less important, of course, but it would be desirable to increase the number of data for small earthquakes. This will be accomplished when we add all the recently recorded earthquakes to the data set.

*Few Class A data.* Ground-motion predictions for Class A are not as well determined as for the other classes because there are very few Class A sites. In the response-spectral data set there are 11 Class A sites, 49 Class B sites, and 46 Class C sites. (The total number of sites is less than the total number of records because some sites recorded more than one earthquake.) The residual plots for class A data (Figure 9) suggest that the predictions may be somewhat low within about 12 km for peak acceleration. When we add all the

10

recently recorded earthquakes to the data set, we will increase the number of Class A data, but there will always be fewer data in Class A than in the other classes.

*Poor distribution of Class D sites.* We did not include records from Class D sites in the data analysis, because those records were available from only one earthquake (Loma Prieta) and only from a limited area and we could not presume that they constituted a representative sample. This situation will not improve until more recordings are made at Class D sites. The Loma Prieta Class D recordings were used by Joyner *et al.* (1994) to estimate site effects on response spectral values by comparison with recordings at other nearby sites.

*Effect of site conditions on short-period motion.* The equations developed from our current data set show differences between site classes for peak acceleration and for response spectra at all periods, while the earlier equations showed little or no difference for peak acceleration or for response spectra at periods 0.3 sec and smaller. The change is the result of adding new data, and it is an improvement in the sense that the new data set includes a broader range of site conditions. The particular way in which site conditions affect short-period motions, however, may depend on variables not included in the prediction equations. For example, two sites may have the same average shear velocity over the upper 30 m, but they may be underlain by different thicknesses of attenuating material. For a large enough thickness, the effect of anelastic attenuation on short-period motions may largely offset, or even reverse, the effect of amplification. When we add all the recently-recorded earthquakes to the data set and compile all the available geologic site data, we will try adding a variable representing the thickness of attenuating material to the equations.

*Averaging velocity over 30 m.* The use of average shear-wave velocity to a depth of 30 m as a variable to characterize site conditions is a choice dictated by the relative unavailability of velocity data for greater depths. The ideal parameter would be average shear-wave velocity to a depth of one-quarter wavelength for the period of interest, as was used by Joyner and Fumal (1984; see also Boore and Joyner, 1991). By the quarter-wavelength rule, 30 m is the appropriate depth for periods less than 0.16 sec for Class A, periods between 0.16 and 0.33 sec for Class B, and periods between 0.33 and 0.67 sec for Class C. The use of shear-wave velocity averaged over 30 m may work reasonably well for other depths and periods, because it will have a high correlation with the average over greater depths. We hope, however, to develop estimates of average shear-wave velocity to greater depths at a sufficient number of sites so that we can ultimately provide ground-motion prediction equations in terms of average shear-wave velocity to a depth of one-quarter wavelength.

11

*Distance limitations.* There are very few recordings in the data set for distances greater than 100 km, and we recommend that the equations not be used for greater distances. Such a limitation is inherent in the strong-motion data set as long as it is dominated by conventional triggered instruments. In our future work we hope to extend the range of our predictions to larger distances by using weak-motion data recorded on seismographic networks to obtain the attenuation of ground motion with distance in combination with stochastic methods (e.g., Hanks and McGuire, 1981; Boore, 1983) to define the magnitude scaling. The magnitude scaling at distances beyond about 100 km may be somewhat greater than at closer distances for two reasons: the periods controlling the oscillator response may increase because of anelastic attenuation, and the energy radiated by the earthquake may be spread over a longer duration. An example of the distance-dependence of the magnitude scaling can be seen in Figure 9 of Atkinson and Boore (1990).

*Basin-generated surface waves.* Surface waves have been recorded by strong-motion instruments at sites in deep sedimentary basins (Hanks, 1975). These waves arrive later than the $S$ body waves and have periods in the general range of 3–10 sec. In some, perhaps most, cases these waves are generated at the margins of the sedimentary basins by conversion from body waves in the high-velocity material bounding the basin (Vidale and Helmberger, 1988; Frankel *et al.*, 1991). At some sites the largest amplitudes at long periods may be due to surface waves. Surface waves are probably not significant for the periods covered by the equations in BJF93 and the present report (two seconds and less), but they represent an important issue in ground-motion prediction.

*Effect of distance cutoffs that are independent of geology and azimuth.* The limits on the distance range within which our equations may be used for predicting ground motion are made more severe by our attempt to avoid bias due to instruments that do not trigger. To avoid that bias, we exclude from the data set for each earthquake all records obtained at distances equal to or greater than the closest operational instrument that did not trigger or that triggered on the $S$ wave. We use different cutoff distances for stations employing a trigger sensitive to horizontal motion and those with a trigger sensitive to vertical motion, but for simplicity we use cutoff distances independent of geologic site conditions and independent of azimuth (see BJF93). Because amplitude depends on site conditions and on azimuth through the effects of radiation pattern and directivity, the use of cutoff distances independent of geology and azimuth may result in the unnecessary exclusion of records. We choose simplicity and objectivity, however, over increasing the number of records in the data set, and we believe avoiding bias is far more important than

increasing the number of data. Alternative methods of avoiding bias are available that do not require the exclusion of records (Toro, 1981; McLaughlin, 1991). Although these methods add significantly to the complexity of the analysis we may consider these methods in our future work. They will become largely unnecessary, however, if we have functions giving ground-motion distance dependence developed by stochastic methods with the help of data other than strong-motion data, as described above.

## ERRATA FOR BJF93

Here is a list of typographical errors and omissions in BJF93 known to us at this time:

p. 4, l. 2: Delete extra ".".

p. 5, l. 10 from bottom: Records for which only a single horizontal component was available were not deleted if the other component was not operational.

p. 7, l. 4: Replace extra "i" with "n" in "wiinowed".

p. 11, last line: Replace "Agency" with "Commission".

Tables 4 and 5: The Anderson Dam recording of the Loma Prieta earthquake was obtained at the downstream site.

Table 6: The latitude of Hole 131 (Gilroy #7) should be 37.033.

Table 6: The information used to assign average shear-wave velocity to those boreholes with a reference to "EPRI/CUREE" was preliminary, and has been superseded by the report by Thiel and Schneider (1993). The average velocity at all sites has changed, and in four cases the new shear-wave velocities have produced a change in site class. Table 10 contains those sites that change class, and Table 11 gives updated borehole information (including some sites not used in the regression analysis). We determined that the changes had no significant effect on the equations in BJF93, and for that reason we chose not to include corrected equations in this paper.

## ACKNOWLEDGMENTS

We wish to thank Norm Abrahamson and Ken Campbell for their comments, Charles Mueller for his review of the manuscript, and S. Midorikawa for providing data plotted in

13

## REFERENCES

Aki, K. and P. G. Richards (1980). *Quantitative Seismology Theory and Methods* 1, 557 p., W. H. Freeman and Company.

Algermissen S. T., J. W. Dewey, C. J. Langer, and W. H. Dillinger (1974). The Managua, Nicaragua, earthquake of December 23, 1972: Location, focal mechanism, and intensity distribution, *Bull. Seism. Soc. Am.* 64, 993–1004

Allen, C. R. and J. M. Nordquist (1972). Foreshock, main shock, and larger aftershocks of the Borrego Mountain earthquake, *U. S. Geol. Surv. Prof. Paper 787*, 16–23.

Archuleta, R. J. (1984). A faulting model for the 1979 Imperial Valley earthquake, *J. Geophys. Res.* 89, 4559–4585.

Atkinson, G. M. and D. M. Boore (1990). Recent trends in ground motion and spectral response relations for North America, *Earthquake Spectra* 6, 15–35.

Boore, D. M. (1983). Stochastic simulation of high-frequency ground motions based on seismological models of the radiated spectra, *Bull. Seism. Soc. Am.* 73, 1865–1894.

Boore, D. M. and D. J. Stierman (1976). Source parameters of the Pt. Mugu, California, earthquake of February 21, 1973, *Bull. Seism. Soc. Am.* 66, 385–404.

Boore, D. M. and W. B. Joyner (1991). Estimation of ground motion at deep-soil sites in eastern North America, *Bull. Seism. Soc. Am.* 81, 2167–2185.

Boore, D. M., W. B. Joyner, and T. E. Fumal (1993). Estimation of response spectra and peak accelerations from western North American earthquakes: An interim report, *U. S. Geol. Surv. Open-File Rept. 93-509*, 72 pp.

Borcherdt, R. D. (1994). Simplified site classes and empirical amplification factors for site-dependent code provisions, *Proceedings NCEER/SEAOC/BSSC Workshop on Site Response During Earthquakes and Seismic Code Provisions*, University of Southern California, November 18–20, 1992, (in press).

Brillinger, D. R. and H. K. Preisler (1984). An exploratory analysis of the Joyner-Boore attenuation data, *Bull. Seism. Soc. Am.* **74**, 1441–1450.

Brillinger, D. R. and H. K. Preisler (1985). Further analysis of the Joyner-Boore attenuation data, *Bull. Seism. Soc. Am.* **75**, 611–614.

Campbell, K. W. and Y. Bozorgnia (1994). Near-source attenuation of peak horizontal acceleration from worldwide accelerograms recorded from 1957 to 1993, Proc. Fifth U. S. National Conference on Earthquake Engineering, Chicago, Illinois, July 10-14, 1994 (in press).

Cockerham, R. S., F. W. Lester, and W. L. Ellsworth (1980). A preliminary report on the Livermore Valley earthquake sequence January 24–February 26, 1980, *U. S. Geol. Surv. Open-File Rept. 80-714.*

Corbett, E. J. and C. E. Johnson (1982). The Santa Barbara, California, earthquake of 13 August 13 1978, *Bull. Seism. Soc. Am.* **72**, 2201-2226.

Donovan, N. C. and A. E. Bornstein (1978). Uncertainties in seismic risk procedures, *Proc. Am. Soc. Civil Eng., J. Geotech. Eng. Div.* **104**, 869–887.

Dunbar, W. S., D. M. Boore, and W. Thatcher (1980), Pre-, co-, and postseismic strain changes associated with the 1952 $M_L = 7.2$ Kern County, California, earthquake, *Bull. Seism. Soc. Am.* **70**, 1893–1905.

Frankel, A., S. Hough, P. Friberg, and R. Busby (1991). Observations of Loma Prieta aftershocks from a dense array in Sunnyvale, California *Bull. Seism. Soc. Am.* **81**, 1900–1922.

Given, D. D. (1983). Seismicity and structure of the trifurcation in the San Jacinto fault zone, southern California, *M.S. thesis, Cal. State University, Los Angeles*, 73 p.

Hanks, T. C. (1975). Strong ground motion of the San Fernando, California, earthquake: ground displacements, *Bull. Seism. Soc. Am.* **65**, 193–225.

Hanks, T. C. and R. K. McGuire (1981). The character of high frequency strong ground motion, *Bull. Seism. Soc. Am.* **71**, 2071–2095.

Hasegawa, H. S., J. C. Lahr, and C. D. Stephens (1980). Fault parameters of the St. Elias, Alaska, earthquake of February 28, 1979, *Bull. Seism. Soc. Am.* **70**, 1651–1660.

Heaton, T. H. (1982). The 1971 San Fernando earthquake: A double event?, *Bull. Seism. Soc. Am.* **72**, 2037–2062.

Idriss, I. M. (1985). Evaluating seismic risk in engineering practice, *Proc. Eleventh Internat. Conf. on Soil Mech. and Foundation Eng.*, August 12–16, 1985, San Francisco, California, **1**, 255–320, A. A. Balkema, Rotterdam.

Joyner, W.B. and D.M. Boore (1981). Peak acceleration and velocity from strong-motion records including records from the 1979 Imperial Valley, California, earthquake, *Bull. Seism. Soc. Am.* **71**, 2011–2038.

Joyner, W.B. and D.M. Boore (1982). Prediction of earthquake response spectra, *U. S. Geol. Surv. Open-File Rept. 82-977*, 16 p.

Joyner, W.B. and D.M. Boore (1993). Methods for regression analysis of strong-motion data, *Bull. Seism. Soc. Am.* **83**, 469–487.

Joyner, W. B. and D. M. Boore (1994). Errata, *Bull. Seism. Soc. Am.* **84**, (in press).

Joyner, W. B. and T. E. Fumal (1984). Use of measured shear-wave velocity for predicting geologic site effects on strong ground motion, *Proc. Eighth World Conf. on Earthquake Eng. (San Francisco)* **2**, 777–783.

Joyner, W. B., T. E. Fumal, and G. Glassmoyer (1994). Empirical spectral response ratios for strong-motion data from the 1989 Loma Prieta, California, earthquake, *Proceedings NCEER/SEAOC/BSSC Workshop on Site Response During Earthquakes and Seismic Code Provisions*, Los Angeles, November 18–20, 1992 (in press).

Kanamori, H., H. K. Thio, D. Dreger, E. Hauksson, and T. Heaton (1992). Initial investigation of the Landers, California, earthquake of 28 June 1992 using TERRAscope, *Geophys. Res. Lett.* **19**, 2267–2270.

Langston, C. A. (1978). The February 9, 1971 San Fernando earthquake: A study of source finiteness in teleseismic body waves, *Bull. Seism. Soc. Am.* **68**, 1–29.

Lee, W. H. K. (1974). A preliminary study of the Hollister earthquake of November 28, 1974 and its major aftershocks, (unpublished manuscript dated December 6, 1974).

Liu, H-L and D. V. Helmberger (1983). The near-source ground motion of the 6 August 1979 Coyote Lake, California, earthquake, *Bull. Seism. Soc. Am.* **73**, 201–218.

McEvilly, T. V. (1966). Preliminary seismic data June-July, 1966, Monterey and San Luis Obispo Counties, California, preliminary report, *Bull. Seism. Soc. Am.* **56**, 967–971.

McLaughlin, K. L. (1991). Maximum likelihood estimation of strong-motion attenuation relationships, *Spectra* **7**, 267–279.

Oppenheimer, D., G. Beroza, G. Carver, L. Dengler, J. Eaton, L. Gee, F. Gonzalez, A. Jayko, W. H. Li, M. Lisowski, M. Magee, G. Marshall, M. Murray, R. McPherson, B. Romanowicz, K. Satake, R. Simpson, P. Somerville, R. Stein, and D. Valentine (1993). The Cape Mendocino, California, earthquakes of April 1992: Subduction at the triple junction, *Science* **261**, 433–438.

Press, W.H., B.P. Flannery, S.A. Teukolsky, and W.T. Vetterling (1986). *Numerical Recipes, the Art of Scientific Computing*, Cambridge University Press, Cambridge, U.K.

Richter, C. F. (1958). *Elementary Seismology*, W. H. Freeman and Company, San Francisco, 768 pp.

Schell, M. M. and L. J. Ruff (1986). Southeastern Alaska tectonics: Source process of the large 1972 Sitka earthquake (abs), *Eos (Trans. Amer. Geophys. Un.)* **67**, 304.

Searle, S. R. (1971). *Linear Models*, Wiley, New York, 532 pp.

Stein, R. S. and W. Thatcher (1981). Seismic and aseismic deformation associated with the 1952 Kern County, California, earthquake and relationship to the quaternary history of the White Wolf fault, *J. Geophys. Res.* **86**, 4913–4928.

Thiel Jr., C. C. and J. F. Schneider (1993). Investigations of Thirty-Three Loma Prieta Earthquake Strong Motion Recording Sites, final report of project sponsored by the Building Contractors Society of Japan and the Electric Power Research Institute, California Universities for Research in Earthquake Engineering (CUREe), Dept. of

Civil Engineering, Stanford Univ., Stanford, Calif.

Toro, G. R. (1981). Biases in seismic ground motion prediction, Massachusetts Institute of Technology, Department of Civil Eng. Res. Rept. R81-22, Cambridge, Massachusetts, 133 p.

Uhrhammer, R. A. (1981). The Pacifica earthquake of 28 April 1979, *Bull. Seism. Soc. Am.* **71**, 1161–1172.

Vidale, J. E. and D. V. Helmberger (1988). Elastic finite-difference modeling of the 1971 San Fernando, California, earthquake, *Bull. Seism. Soc. Am.* **78**, 122–141.

Wallace, T. C., A. Velasco, J. Zhang, and T. Lay (1991). A broadband seismological investigation of the 1989 Loma Prieta, California, earthquake: Evidence for deep slow slip?, *Bull. Seism. Soc. Am.* **81**, 1622–1646.

Whitcomb, J. H. (1971). Fault-plane solutions of the February 9, 1971, San Fernando earthquake and some aftershocks, *U. S. Geol. Surv. Prof. Paper 733*, 30–32.

Youngs, R. R., N. Abrahamson, F. Makdisi, and K. Sadigh (1994). Magnitude-dependent variance of peak ground acceleration, *Bull. Seism. Soc. Am.* **84**, (in press).

Table 1.  Records used in the development of the equations for response spectra as a continuous function of average shear velocity.

| DATE | EARTHQUAKE | M | DIST | STATION | LAT. | LONG. | G | AVGVEL | HOLE | SOURCE |
|---|---|---|---|---|---|---|---|---|---|---|
| 19-May-40 | Imperial Vall | 7.00 | 12.0 | El Centro Array Sta 9 | 32.794 | 115.549 | C | 213 | 107 | n |
| 21-Jul-52 | Kern County | 7.40 | 42.0 | Taft | 35.150 | 119.460 | B | 429 | 201 | n |
| 21-Jul-52 | Kern County | 7.40 | 85.0 | Santa Barbara | 34.420 | 119.700 | B | 508 | 96 | n |
| 21-Jul-52 | Kern County | 7.40 | 109.0 | Pasadena - Athenaeum | 34.140 | 118.120 | B | 417 | 92 | n |
| 21-Jul-52 | Kern County | 7.40 | 107.0 | Hollywood Storage Bldg PE Lo | 34.090 | 118.340 | C | 318 | 63 | n |
| 22-Mar-57 | Daly City | 5.30 | 8.0 | San Fran.: Golden Gate Park | 37.770 | 122.480 | A | 783 | 173 | n |
| 28-Jun-66 | Parkfield | 6.10 | 16.1 | Cholame-Shandon: Temblor | 35.710 | 120.170 | B | 509 | 200 | n |
| 28-Jun-66 | Parkfield | 6.10 | 6.6 | Parkfield: Cholame 2 | 35.733 | 120.288 | C | 194 | 228 | n |
| 28-Jun-66 | Parkfield | 6.10 | 9.3 | Parkfield: Cholame 5W | 35.697 | 120.328 | C | 278 | 197 | n |
| 28-Jun-66 | Parkfield | 6.10 | 13.0 | Parkfield: Cholame 8W | 35.671 | 120.359 | C | 260 | 198 | n |
| 9-Apr-68 | Borrego Mount | 6.60 | 45.0 | El Centro Array Sta 9 | 32.794 | 115.549 | C | 213 | 107 | n |
| 9-Feb-71 | San Fernando | 6.60 | 17.0 | Lake Hughes Sta 12 | 34.570 | 118.560 | B | 600 | 86 | n |
| 9-Feb-71 | San Fernando | 6.60 | 25.7 | Pasadena - Athenaeum | 34.140 | 118.120 | B | 417 | 92 | n |
| 9-Feb-71 | San Fernando | 6.60 | 60.7 | Wrightwood | 34.360 | 117.630 | B | 482 | 88 | n |
| 9-Feb-71 | San Fernando | 6.60 | 19.6 | Lake Hughes Sta 4 | 34.650 | 118.478 | C | 351 | 71 | n |
| 6-Aug-79 | Coyote Lake | 5.80 | 9.1 | Gilroy Array 1 | 36.973 | 121.572 | A | 1415 | 192 | n |
| 6-Aug-79 | Coyote Lake | 5.80 | 1.2 | Gilroy Array 6 | 37.026 | 121.484 | B | 714 | 196 | n |
| 6-Aug-79 | Coyote Lake | 5.80 | 3.7 | Gilroy Array 4 | 37.005 | 121.522 | C | 223 | 195 | n |
| 6-Aug-79 | Coyote Lake | 5.80 | 5.3 | Gilroy Array 3 | 36.987 | 121.536 | C | 306 | 194 | n |
| 6-Aug-79 | Coyote Lake | 5.80 | 7.4 | Gilroy Array 2 | 36.982 | 121.556 | C | 309 | 193 | n |
| 15-Oct-79 | Imperial Vall | 6.50 | 14.0 | Parachute Test Site | 32.929 | 115.699 | B | 370 | 116 | n |
| 15-Oct-79 | Imperial Vall | 6.50 | .6 | El Centro Array Sta 7 | 32.829 | 115.504 | C | 211 | 105 | n |
| 15-Oct-79 | Imperial Vall | 6.50 | 1.3 | El Centro Array Sta 6 | 32.839 | 115.487 | C | 201 | 104 | n |
| 15-Oct-79 | Imperial Vall | 6.50 | 2.6 | Bonds Corner | 32.693 | 115.338 | C | 224 | 97 | n |
| 15-Oct-79 | Imperial Vall | 6.50 | 3.8 | El Centro Array Sta 8 | 32.810 | 115.530 | C | 205 | 106 | n |
| 15-Oct-79 | Imperial Vall | 6.50 | 4.0 | El Centro Array Sta 5 | 32.855 | 115.466 | C | 207 | 103 | n |
| 15-Oct-79 | Imperial Vall | 6.50 | 5.1 | El Centro: Differential Arra | 32.796 | 115.535 | C | 200 | 112 | n |
| 15-Oct-79 | Imperial Vall | 6.50 | 6.8 | El Centro Array Sta 4 | 32.864 | 115.432 | C | 211 | 102 | n |
| 15-Oct-79 | Imperial Vall | 6.50 | 7.5 | Holtville | 32.812 | 115.377 | C | 201 | 99 | n |
| 15-Oct-79 | Imperial Vall | 6.50 | 8.5 | El Centro Array Sta 10 | 32.780 | 115.567 | C | 203 | 108 | n |
| 15-Oct-79 | Imperial Vall | 6.50 | 8.5 | Brawley | 32.991 | 115.512 | C | 210 | 114 | n |
| 15-Oct-79 | Imperial Vall | 6.50 | 12.6 | El Centro Array Sta 11 | 32.752 | 115.594 | C | 196 | 109 | n |
| 15-Oct-79 | Imperial Vall | 6.50 | 16.0 | El Centro Array Sta 2 | 32.916 | 115.366 | C | 190 | 100 | n |
| 15-Oct-79 | Imperial Vall | 6.50 | 18.0 | El Centro Array Station 12 | 32.718 | 115.637 | C | 210 | 110 | n |
| 15-Oct-79 | Imperial Vall | 6.50 | 22.0 | El Centro Array Sta 13 | 32.709 | 115.683 | C | 252 | 111 | n |
| 15-Oct-79 | Imperial Vall | 6.50 | 23.0 | Calipatria | 33.130 | 115.520 | C | 197 | 117 | n |
| 18-Oct-89 | Loma Prieta | 6.92 | 10.5 | Gilroy Array 1 | 36.973 | 121.572 | A | 1415 | 192 | c |
| 18-Oct-89 | Loma Prieta | 6.92 | 42.7 | Monterey City Hall | 36.597 | 121.897 | A | 763 | 209 | c |
| 18-Oct-89 | Loma Prieta | 6.92 | 67.6 | S. San Fran.: Sierra Pt. | 37.674 | 122.388 | A | 1020 | 220 | c |

| Date | Event | Dist | Mag | Station | Lat | Long | | AVGVEL | | |
|---|---|---|---|---|---|---|---|---|---|---|
| 18-Oct-89 | Loma Prieta | 6.92 | 0.0 | Corralitos | 37.046 | 121.803 | B | 460 | 130 | c |
| 18-Oct-89 | Loma Prieta | 6.92 | 19.9 | Gilroy Array 6 | 37.026 | 121.484 | B | 714 | 196 | c |
| 18-Oct-89 | Loma Prieta | 6.92 | 20.0 | Anderson Dam: Downstream | 37.166 | 121.628 | B | 506 | 142 | u |
| 18-Oct-89 | Loma Prieta | 6.92 | 34.1 | SAGO South A | 36.753 | 121.396 | B | 612 | 211 | c |
| 18-Oct-89 | Loma Prieta | 6.92 | 36.1 | Calaveras Reservoir South | 37.452 | 121.807 | B | 482 | 143 | u |
| 18-Oct-89 | Loma Prieta | 6.92 | 38.7 | Woodside | 37.429 | 122.258 | B | 455 | 132 | c |
| 18-Oct-89 | Loma Prieta | 6.92 | 42.0 | Mission San Jose | 37.530 | 121.919 | B | 368 | 224 | c |
| 18-Oct-89 | Loma Prieta | 6.92 | 46.4 | APEEL Array Sta 9 | 37.478 | 122.321 | B | 454 | 1 | u |
| 18-Oct-89 | Loma Prieta | 6.92 | 46.5 | APEEL Array Sta 7 | 37.484 | 122.313 | B | 435 | 164 | c |
| 18-Oct-89 | Loma Prieta | 6.92 | 46.6 | APEEL Array Sta 10 | 37.465 | 122.343 | B | 401 | 12 | c |
| 18-Oct-89 | Loma Prieta | 6.92 | 48.7 | Belmont | 37.512 | 122.308 | B | 628 | 210 | c |
| 18-Oct-89 | Loma Prieta | 6.92 | 49.9 | Sunol Fire Station | 37.597 | 121.880 | B | 405 | 141 | c |
| 18-Oct-89 | Loma Prieta | 6.92 | 53.7 | Bear Valley Sta 5 | 36.673 | 121.195 | B | 391 | 145 | u |
| 18-Oct-89 | Loma Prieta | 6.92 | 56.0 | APEEL Array Sta 3E | 37.657 | 122.061 | B | 522 | 158 | c |
| 18-Oct-89 | Loma Prieta | 6.92 | 58.7 | Hayward City Hall: N. FF | 37.679 | 122.082 | B | 743 | 137 | u |
| 18-Oct-89 | Loma Prieta | 6.92 | 8.6 | Capitola | 36.974 | 121.952 | C | 289 | 219 | c |
| 18-Oct-89 | Loma Prieta | 6.92 | 12.1 | Gilroy Array 2 | 36.982 | 121.556 | C | 309 | 193 | c |
| 18-Oct-89 | Loma Prieta | 6.92 | 14.0 | Gilroy Array 3 | 36.987 | 121.536 | C | 306 | 194 | c |
| 18-Oct-89 | Loma Prieta | 6.92 | 15.8 | Gilroy Array 4 | 37.005 | 121.522 | C | 223 | 195 | c |
| 18-Oct-89 | Loma Prieta | 6.92 | 24.3 | Gilroy Array 7 | 37.033 | 121.434 | C | 333 | 131 | c |
| 18-Oct-89 | Loma Prieta | 6.92 | 25.4 | Hollister: Airport | 36.888 | 121.413 | C | 218 | 147 | c |
| 18-Oct-89 | Loma Prieta | 6.92 | 27.0 | Agnew | 37.397 | 121.952 | C | 264 | 221 | c |
| 18-Oct-89 | Loma Prieta | 6.92 | 27.5 | Sunnyvale | 37.402 | 122.024 | C | 268 | 136 | u |
| 18-Oct-89 | Loma Prieta | 6.92 | 29.3 | Halls Valley | 37.338 | 121.714 | C | 265 | 230 | c |
| 18-Oct-89 | Loma Prieta | 6.92 | 34.8 | Palo Alto: 2-Story Office Bl | 37.453 | 122.112 | C | 207 | 128 | c |
| 18-Oct-89 | Loma Prieta | 6.92 | 35.0 | Stanford: SLAC Test Lab | 37.419 | 122.205 | C | 344 | 134 | u |
| 18-Oct-89 | Loma Prieta | 6.92 | 42.4 | Fremont | 37.535 | 121.929 | C | 283 | 140 | c |
| 18-Oct-89 | Loma Prieta | 6.92 | 50.9 | Bear Valley Sta 12 | 36.658 | 121.249 | C | 330 | 144 | u |
| 18-Oct-89 | Loma Prieta | 6.92 | 56.3 | APEEL Array Sta 2E | 37.657 | 122.083 | C | 276 | 150 | c |
| 18-Oct-89 | Loma Prieta | 6.92 | 63.2 | San Fran.: Airport | 37.622 | 122.398 | C | 224 | 123 | c |
| 18-Oct-89 | Loma Prieta | 6.92 | 67.3 | Bear Valley Sta 10 | 36.532 | 121.143 | C | 311 | 146 | u |

AVGVEL is the time-weighted shear velocity averaged over the upper 30 m, in units
  of meters/second.
SOURCE is expanded in the footnote to Table 5 in BJF93.

Table 2. Smoothed coefficients for response spectra (psv in cm/s; sa in g; shear velocity in m/s)

| T(s) | BSA | random, 02% BV | VA | random, 05% BV | VA | random, 10% BV | VA | random, 20% BV | VA | larger, 02% BV | VA | larger, 05% BV | VA | larger, 10% BV | VA | larger, 20% BV | VA |
|---|---|---|---|---|---|---|---|---|---|---|---|---|---|---|---|---|---|
| .10 | -1.193 | -.191 | 970 | -.212 | 1110 | -.222 | 1310 | -.251 | 1510 | -.188 | 950 | -.207 | 1080 | -.215 | 1220 | -.232 | 1540 |
| .11 | -1.234 | -.189 | 1160 | -.211 | 1290 | -.225 | 1470 | -.255 | 1620 | -.184 | 1160 | -.206 | 1280 | -.218 | 1430 | -.234 | 1720 |
| .12 | -1.272 | -.191 | 1340 | -.215 | 1450 | -.230 | 1600 | -.261 | 1710 | -.185 | 1370 | -.209 | 1470 | -.224 | 1610 | -.238 | 1870 |
| .13 | -1.307 | -.197 | 1500 | -.221 | 1600 | -.238 | 1710 | -.269 | 1790 | -.190 | 1560 | -.214 | 1640 | -.230 | 1760 | -.243 | 2000 |
| .14 | -1.339 | -.205 | 1640 | -.228 | 1720 | -.247 | 1810 | -.277 | 1850 | -.196 | 1730 | -.221 | 1790 | -.238 | 1900 | -.250 | 2110 |
| .15 | -1.369 | -.214 | 1760 | -.238 | 1820 | -.257 | 1880 | -.287 | 1900 | -.204 | 1870 | -.229 | 1910 | -.247 | 2010 | -.257 | 2200 |
| .16 | -1.397 | -.225 | 1860 | -.248 | 1910 | -.267 | 1950 | -.296 | 1940 | -.214 | 2000 | -.238 | 2020 | -.256 | 2110 | -.265 | 2280 |
| .17 | -1.423 | -.236 | 1950 | -.258 | 1980 | -.278 | 2000 | -.306 | 1970 | -.224 | 2100 | -.247 | 2110 | -.265 | 2190 | -.273 | 2330 |
| .18 | -1.448 | -.248 | 2020 | -.270 | 2040 | -.289 | 2040 | -.316 | 1990 | -.235 | 2190 | -.257 | 2180 | -.274 | 2250 | -.282 | 2380 |
| .19 | -1.472 | -.260 | 2070 | -.281 | 2080 | -.300 | 2070 | -.326 | 2010 | -.246 | 2260 | -.267 | 2240 | -.284 | 2300 | -.290 | 2420 |
| .20 | -1.494 | -.273 | 2120 | -.292 | 2120 | -.311 | 2080 | -.336 | 2020 | -.257 | 2320 | -.277 | 2290 | -.293 | 2340 | -.299 | 2440 |
| .22 | -1.535 | -.298 | 2170 | -.315 | 2160 | -.333 | 2110 | -.355 | 2040 | -.280 | 2390 | -.297 | 2350 | -.311 | 2390 | -.316 | 2470 |
| .24 | -1.573 | -.322 | 2180 | -.338 | 2180 | -.355 | 2110 | -.374 | 2040 | -.302 | 2430 | -.316 | 2380 | -.332 | 2410 | -.332 | 2470 |
| .26 | -1.608 | -.347 | 2200 | -.360 | 2170 | -.375 | 2100 | -.392 | 2030 | -.325 | 2440 | -.336 | 2380 | -.346 | 2400 | -.348 | 2460 |
| .28 | -1.640 | -.370 | 2190 | -.381 | 2160 | -.395 | 2080 | -.409 | 2020 | -.346 | 2430 | -.354 | 2370 | -.363 | 2390 | -.363 | 2440 |
| .30 | -1.670 | -.392 | 2160 | -.401 | 2130 | -.413 | 2060 | -.425 | 2000 | -.366 | 2390 | -.372 | 2340 | -.378 | 2360 | -.377 | 2410 |
| .32 | -1.698 | -.413 | 2130 | -.420 | 2100 | -.431 | 2030 | -.440 | 1980 | -.386 | 2360 | -.388 | 2310 | -.393 | 2330 | -.391 | 2370 |
| .34 | -1.725 | -.433 | 2090 | -.438 | 2070 | -.448 | 2000 | -.455 | 1960 | -.405 | 2310 | -.404 | 2280 | -.407 | 2290 | -.404 | 2340 |
| .36 | -1.749 | -.452 | 2050 | -.456 | 2030 | -.463 | 1970 | -.468 | 1940 | -.422 | 2260 | -.420 | 2230 | -.420 | 2250 | -.417 | 2300 |
| .38 | -1.773 | -.470 | 2000 | -.472 | 2000 | -.478 | 1940 | -.481 | 1920 | -.439 | 2210 | -.434 | 2190 | -.433 | 2210 | -.428 | 2260 |
| .40 | -1.795 | -.487 | 1960 | -.487 | 1950 | -.492 | 1910 | -.493 | 1900 | -.455 | 2170 | -.448 | 2150 | -.445 | 2170 | -.439 | 2220 |
| .42 | -1.816 | -.504 | 1920 | -.502 | 1920 | -.506 | 1870 | -.505 | 1870 | -.470 | 2110 | -.461 | 2100 | -.456 | 2130 | -.450 | 2190 |
| .44 | -1.836 | -.519 | 1880 | -.516 | 1880 | -.518 | 1850 | -.516 | 1850 | -.485 | 2070 | -.473 | 2070 | -.467 | 2090 | -.460 | 2150 |
| .46 | -1.856 | -.533 | 1840 | -.529 | 1850 | -.530 | 1820 | -.526 | 1840 | -.498 | 2020 | -.485 | 2020 | -.477 | 2050 | -.469 | 2110 |
| .48 | -1.874 | -.547 | 1800 | -.541 | 1820 | -.541 | 1790 | -.535 | 1820 | -.511 | 1980 | -.496 | 1990 | -.486 | 2010 | -.478 | 2080 |
| .50 | -1.892 | -.560 | 1760 | -.553 | 1780 | -.552 | 1760 | -.545 | 1790 | -.523 | 1930 | -.506 | 1950 | -.495 | 1980 | -.487 | 2050 |
| .55 | -1.933 | -.589 | 1680 | -.579 | 1710 | -.575 | 1700 | -.565 | 1750 | -.550 | 1840 | -.530 | 1860 | -.516 | 1900 | -.506 | 1980 |
| .60 | -1.971 | -.615 | 1610 | -.602 | 1640 | -.596 | 1650 | -.583 | 1710 | -.574 | 1750 | -.551 | 1790 | -.534 | 1830 | -.522 | 1910 |
| .65 | -2.006 | -.637 | 1550 | -.622 | 1590 | -.614 | 1610 | -.598 | 1680 | -.594 | 1690 | -.569 | 1730 | -.549 | 1770 | -.537 | 1860 |
| .70 | -2.038 | -.655 | 1500 | -.639 | 1550 | -.629 | 1570 | -.611 | 1650 | -.611 | 1630 | -.584 | 1680 | -.563 | 1730 | -.550 | 1810 |
| .75 | -2.068 | -.671 | 1460 | -.653 | 1510 | -.642 | 1540 | -.622 | 1630 | -.626 | 1580 | -.598 | 1640 | -.575 | 1690 | -.561 | 1770 |
| .80 | -2.096 | -.685 | 1420 | -.666 | 1480 | -.653 | 1510 | -.632 | 1610 | -.639 | 1540 | -.609 | 1600 | -.585 | 1650 | -.570 | 1740 |
| .85 | -2.122 | -.697 | 1390 | -.676 | 1450 | -.662 | 1490 | -.640 | 1590 | -.650 | 1510 | -.619 | 1580 | -.594 | 1630 | -.578 | 1710 |
| .90 | -2.147 | -.706 | 1370 | -.685 | 1430 | -.669 | 1480 | -.647 | 1570 | -.659 | 1490 | -.628 | 1560 | -.602 | 1610 | -.585 | 1690 |
| .95 | -2.171 | -.714 | 1350 | -.692 | 1420 | -.676 | 1470 | -.652 | 1560 | -.666 | 1470 | -.635 | 1540 | -.608 | 1590 | -.591 | 1680 |
| 1.00 | -2.193 | -.721 | 1340 | -.698 | 1410 | -.681 | 1460 | -.657 | 1550 | -.672 | 1460 | -.641 | 1530 | -.614 | 1580 | -.596 | 1670 |
| 1.10 | -2.234 | -.729 | 1330 | -.706 | 1400 | -.688 | 1460 | -.664 | 1540 | -.679 | 1460 | -.650 | 1530 | -.623 | 1580 | -.604 | 1650 |
| 1.20 | -2.272 | -.733 | 1340 | -.710 | 1400 | -.691 | 1460 | -.667 | 1540 | -.683 | 1470 | -.656 | 1540 | -.628 | 1590 | -.608 | 1650 |
| 1.30 | -2.307 | -.734 | 1350 | -.711 | 1420 | -.691 | 1480 | -.668 | 1540 | -.682 | 1500 | -.658 | 1570 | -.631 | 1610 | -.610 | 1660 |
| 1.40 | -2.339 | -.731 | 1380 | -.709 | 1440 | -.689 | 1500 | -.667 | 1550 | -.679 | 1540 | -.658 | 1610 | -.632 | 1650 | -.611 | 1680 |
| 1.50 | -2.369 | -.725 | 1420 | -.704 | 1480 | -.684 | 1540 | -.664 | 1560 | -.673 | 1600 | -.656 | 1660 | -.631 | 1700 | -.609 | 1710 |
| 1.60 | -2.397 | -.717 | 1480 | -.697 | 1520 | -.678 | 1580 | -.659 | 1580 | -.665 | 1670 | -.652 | 1720 | -.629 | 1750 | -.606 | 1750 |
| 1.70 | -2.423 | -.707 | 1530 | -.689 | 1580 | -.670 | 1630 | -.653 | 1600 | -.655 | 1750 | -.646 | 1800 | -.626 | 1820 | -.602 | 1800 |
| 1.80 | -2.448 | -.695 | 1610 | -.679 | 1640 | -.661 | 1680 | -.646 | 1630 | -.644 | 1850 | -.639 | 1880 | -.621 | 1900 | -.597 | 1850 |
| 1.90 | -2.472 | -.682 | 1690 | -.667 | 1710 | -.650 | 1750 | -.638 | 1660 | -.631 | 1970 | -.631 | 1990 | -.615 | 2000 | -.591 | 1910 |
| 2.00 | -2.494 | -.667 | 1780 | -.655 | 1790 | -.639 | 1820 | -.629 | 1690 | -.616 | 2100 | -.622 | 2100 | -.609 | 2090 | -.584 | 1980 |

The equations are to be used for 5.0 <= M <= 7.7 and d <= 100.0 km

Table 3.  Coefficients of equations for the random and larger horizontal
components of peak acceleration (in g; shear velocity in m/s).

| Component | BV | VA |
|---|---|---|
| random | -.371 | 1400 |
| larger | -.364 | 1390 |

The equations are to be used for $5.0 \leq M \leq 7.7$ and $d \leq 100.0$ km.

22

Table 4. Range of amplitudes defining the middle of the three amplitude classes used in the study of variability.

| T(s) | Middle Amplitude Class (cm/s) |
|------|-------------------------------|
| 0.10 | 2.5 - 7.5 |
| 0.15 | 5.0 - 15.0 |
| 0.24 | 8.0 - 24.0 |
| 0.36 | 12.0 - 36.0 |
| 0.55 | 15.0 - 45.0 |
| 0.85 | 15.0 - 45.0 |
| 1.30 | 15.0 - 45.0 |
| 2.00 | 15.0 - 45.0 |

Table 5. Rake angles

| Quake_Code | Date | Name | Rake | Reference |
|---|---|---|---|---|
| 8 | 5/19/40 | Imperial Valley | 180 | Richter (1958) |
| 18 | 7/21/52 | Kern County | 38 | Dunbar et al. (1980), Stein and Thatcher (1981) |
| 32 | 3/22/57 | Daly City | 999 | Uhrhammer (1981) |
| 50 | 6/28/66 | Parkfield | -160 | McEvilly (1966) |
| 58 | 4/09/68 | Borrego Mountain | 180 | Allen and Nordquist (1972) |
| 64 | 9/12/70 | Lytle Creek | 123 | L. Jones, oral commun., 1993 |
| 65 | 2/09/71 | San Fernando | 76 | Whitcomb (1971), Langston (1978), Heaton (1982) |
| 76 | 7/30/72 | Sitka | 180 | Schell and Ruff (1986) |
| 79 | 12/23/72 | Managua | 0 | Algermissen et al. (1974) |
| 84 | 2/21/73 | Point Mugu | 54 | Boore and Stierman (1976) |
| 97 | 11/28/74 | Hollister | 0 | Lee (1974) |
| 137 | 8/13/78 | Santa Barbara | 57 | Corbett and Johnson (1982) |
| 144 | 2/28/79 | St. Elias | 90 | Hasegawa et al. (1980) and other papers in the same issue |
| 146 | 8/06/79 | Coyote Lake | 177 | Liu and Helmberger (1983) |
| 147 | 10/15/79 | Imperial Valley | 180 | Archuleta (1984) |
| 153 | 1/24/80 | Livermore Valley | -159 | Cockerham et al. (1980) |
| 154 | 1/27/80 | Livermore Valley | -176 | Cockerham et al. (1980) |
| 155 | 2/25/80 | Horse Canyon | -169 | Given (1983) |
| 328 | 10/18/89 | Loma Prieta | 138 | median of values summarized in Table 2 of Wallace et al. (1991) |
| 349 | 4/25/92 | Petrolia | 106 | Oppenheimer et al. (1993) |
| 352 | 6/28/92 | Landers | 176 | Kanamori et al. (1992) |

Table 6. Coefficients for random component as a cubic function of log T for site effect in terms of site classes.

2 percent damped psv (cm/s)

| COEF | C0 | C1 | C2 | C3 |
|------|------|------|------|------|
| B1 | 1.79726 | 2.00791 | -3.74477 | 1.69148 |
| B2 | 0.34064 | -0.09703 | 0.34244 | -0.14241 |
| B3 | -0.11823 | -0.04788 | 0.39058 | -0.23257 |
| H | 6.59550 | 13.59087 | -40.47127 | 23.02134 |
| B5 | -0.95144 | -0.16618 | 0.85766 | -0.48892 |
| B6 | 0.01993 | 0.68233 | -0.58038 | 0.20226 |
| B7 | 0.10640 | 0.53510 | -0.01022 | -0.10863 |
| SIG1 | 0.20487 | -0.08557 | 0.15702 | -0.06530 |
| SIG2 | 0.00650 | -0.00853 | 0.17575 | -0.07055 |
| SIG4 | 0.08664 | 0.12758 | -0.10636 | 0.03900 |

5 percent damped psv (cm/s)

| COEF | C0 | C1 | C2 | C3 |
|------|------|------|------|------|
| B1 | 1.65301 | 1.87615 | -3.17713 | 1.37157 |
| B2 | 0.32667 | -0.22536 | 0.64842 | -0.29982 |
| B3 | -0.09803 | -0.06168 | 0.35352 | -0.20739 |
| H | 6.26923 | 10.59215 | -32.48153 | 18.51690 |
| B5 | -0.93430 | -0.09835 | 0.52386 | -0.28909 |
| B6 | 0.04626 | 0.62911 | -0.57103 | 0.20982 |
| B7 | 0.13633 | 0.48121 | 0.00514 | -0.10607 |
| SIG1 | 0.19117 | -0.05830 | 0.13415 | -0.05913 |
| SIG2 | 0.00266 | 0.05649 | 0.07367 | -0.03324 |
| SIG4 | 0.08263 | 0.11264 | -0.09145 | 0.03751 |

10 percent damped psv (cm/s)

| COEF | C0 | C1 | C2 | C3 |
|------|------|------|------|------|
| B1 | 1.52871 | 1.64978 | -2.52411 | 1.02345 |
| B2 | 0.32446 | -0.27792 | 0.76696 | -0.36207 |
| B3 | -0.08962 | -0.04338 | 0.29700 | -0.17975 |
| H | 5.91207 | 7.42576 | -24.29978 | 13.98860 |
| B5 | -0.91399 | -0.03422 | 0.23345 | -0.11598 |
| B6 | 0.07422 | 0.53054 | -0.47457 | 0.17644 |
| B7 | 0.16035 | 0.44916 | -0.01135 | -0.08832 |
| SIG1 | 0.18009 | -0.03492 | 0.10334 | -0.04458 |
| SIG2 | 0.00695 | 0.06070 | 0.06191 | -0.03321 |
| SIG4 | 0.08368 | 0.07782 | -0.04808 | 0.02375 |

20 percent damped psv (cm/s)

| COEF | C0 | C1 | C2 | C3 |
|------|------|------|------|------|
| B1 | 1.40374 | 1.35854 | -1.88149 | 0.71782 |
| B2 | 0.31205 | -0.17374 | 0.60040 | -0.28394 |
| B3 | -0.08130 | -0.01435 | 0.22199 | -0.14682 |
| H | 5.66338 | 3.63138 | -15.22173 | 9.13430 |
| B5 | -0.89164 | -0.02480 | 0.08096 | -0.02094 |
| B6 | 0.10614 | 0.37912 | -0.23879 | 0.05560 |
| B7 | 0.19135 | 0.37854 | 0.05437 | -0.12154 |
| SIG1 | 0.16865 | 0.00125 | 0.04311 | -0.01424 |
| SIG2 | 0.02248 | 0.00721 | 0.13665 | -0.07236 |
| SIG4 | 0.08637 | 0.06515 | -0.05932 | 0.03907 |

Table 7. Coefficients for larger component as a cubic function of log T for site effect in terms of site classes.

2 percent damped psv (cm/s)

| COEF | C0 | C1 | C2 | C3 |
|------|-----|-----|-----|-----|
| B1 | 1.85796 | 2.10449 | -3.86361 | 1.78453 |
| B2 | 0.33735 | 0.02393 | 0.09652 | -0.01644 |
| B3 | -0.12183 | -0.10318 | 0.44112 | -0.23046 |
| H | 6.47604 | 13.98567 | -41.57274 | 23.87958 |
| B5 | -0.95121 | -0.23530 | 1.04519 | -0.63494 |
| B6 | 0.01260 | 0.68300 | -0.59046 | 0.21780 |
| B7 | 0.10115 | 0.53786 | -0.06125 | -0.06862 |
| SIG1 | 0.20725 | -0.03834 | 0.08832 | -0.03828 |
| SIG2 | -0.00940 | 0.10622 | -0.04323 | 0.05615 |
| SIG4 | 0.00000 | 0.00000 | 0.00000 | 0.00000 |

5 percent damped psv (cm/s)

| COEF | C0 | C1 | C2 | C3 |
|------|-----|-----|-----|-----|
| B1 | 1.70003 | 1.97979 | -3.22270 | 1.40062 |
| B2 | 0.32059 | -0.02727 | 0.24853 | -0.09759 |
| B3 | -0.10401 | -0.15801 | 0.51107 | -0.26515 |
| H | 6.18210 | 10.61936 | -33.14299 | 19.21283 |
| B5 | -0.92131 | -0.22383 | 0.76539 | -0.44561 |
| B6 | 0.03851 | 0.67250 | -0.71115 | 0.30472 |
| B7 | 0.12763 | 0.54306 | -0.20159 | 0.02785 |
| SIG1 | 0.19415 | -0.01519 | 0.07312 | -0.03526 |
| SIG2 | -0.01134 | 0.11701 | -0.05236 | 0.05945 |
| SIG4 | 0.00000 | 0.00000 | 0.00000 | 0.00000 |

10 percent damped psv (cm/s)

| COEF | C0 | C1 | C2 | C3 |
|------|-----|-----|-----|-----|
| B1 | 1.56253 | 1.71556 | -2.43821 | 0.97456 |
| B2 | 0.32384 | -0.06350 | 0.34072 | -0.15288 |
| B3 | -0.10648 | -0.10248 | 0.40387 | -0.21639 |
| H | 5.59958 | 7.90340 | -25.16582 | 14.63759 |
| B5 | -0.88607 | -0.20312 | 0.49729 | -0.26520 |
| B6 | 0.06747 | 0.60771 | -0.69866 | 0.31415 |
| B7 | 0.14209 | 0.58968 | -0.35920 | 0.11128 |
| SIG1 | 0.18659 | -0.02435 | 0.09240 | -0.04125 |
| SIG2 | -0.00998 | 0.08911 | 0.00870 | 0.02598 |
| SIG4 | 0.00000 | 0.00000 | 0.00000 | 0.00000 |

20 percent damped psv (cm/s)

| COEF | C0 | C1 | C2 | C3 |
|------|-----|-----|-----|-----|
| B1 | 1.44367 | 1.41124 | -1.81388 | 0.69053 |
| B2 | 0.32379 | 0.04440 | 0.13760 | -0.05847 |
| B3 | -0.10169 | -0.06309 | 0.31892 | -0.17940 |
| H | 5.43053 | 4.06257 | -16.03367 | 9.71543 |
| B5 | -0.87365 | -0.15375 | 0.29499 | -0.14823 |
| B6 | 0.10701 | 0.37611 | -0.31027 | 0.11562 |
| B7 | 0.17728 | 0.43727 | -0.12623 | -0.00918 |
| SIG1 | 0.17835 | -0.02316 | 0.08933 | -0.03507 |
| SIG2 | 0.00122 | 0.02929 | 0.13472 | -0.05018 |
| SIG4 | 0.00000 | 0.00000 | 0.00000 | 0.00000 |

Table 8. Coefficients for random component as a cubic function of log T for site effect in terms of continuous shear velocity.

2 percent damped psv (cm/s)

| COEF | C0 | C1 | C2 | C3 |
|---|---|---|---|---|
| B1 | 1.79726 | 2.00791 | -3.74477 | 1.69148 |
| B2 | 0.34064 | -0.09703 | 0.34244 | -0.14241 |
| B3 | -0.11823 | -0.04788 | 0.39058 | -0.23257 |
| H | 6.59550 | 13.59087 | -40.47127 | 23.02134 |
| B5 | -0.95144 | -0.16618 | 0.85766 | -0.48892 |
| BV | -0.19059 | 0.11211 | -1.55398 | 0.91181 |
| LOGVA | 2.98711 | 2.03539 | -3.51026 | 1.61535 |
| SIG1 | 0.20487 | -0.08557 | 0.15702 | -0.06530 |
| SIG2 | 0.00650 | -0.00853 | 0.17575 | -0.07055 |
| SIG4 | 0.08664 | 0.12758 | -0.10636 | 0.03900 |

5 percent damped psv (cm/s)

| COEF | C0 | C1 | C2 | C3 |
|---|---|---|---|---|
| B1 | 1.65301 | 1.87615 | -3.17713 | 1.37157 |
| B2 | 0.32667 | -0.22536 | 0.64842 | -0.29982 |
| B3 | -0.09803 | -0.06168 | 0.35352 | -0.20739 |
| H | 6.26923 | 10.59215 | -32.48153 | 18.51690 |
| B5 | -0.93430 | -0.09835 | 0.52386 | -0.28909 |
| BV | -0.21172 | 0.06619 | -1.35085 | 0.79809 |
| LOGVA | 3.04586 | 1.69975 | -2.97445 | 1.37668 |
| SIG1 | 0.19117 | -0.05830 | 0.13415 | -0.05913 |
| SIG2 | 0.00266 | 0.05649 | 0.07367 | -0.03324 |
| SIG4 | 0.08263 | 0.11264 | -0.09145 | 0.03751 |

10 percent damped psv (cm/s)

| COEF | C0 | C1 | C2 | C3 |
|---|---|---|---|---|
| B1 | 1.52871 | 1.64978 | -2.52411 | 1.02345 |
| B2 | 0.32446 | -0.27792 | 0.76696 | -0.36207 |
| B3 | -0.08962 | -0.04338 | 0.29700 | -0.17975 |
| H | 5.91207 | 7.42576 | -24.29978 | 13.98860 |
| B5 | -0.91599 | -0.03422 | 0.23345 | -0.11598 |
| BV | -0.22228 | -0.01615 | -1.13584 | 0.69342 |
| LOGVA | 3.11715 | 1.27112 | -2.32329 | 1.09915 |
| SIG1 | 0.18009 | -0.03492 | 0.10334 | -0.04458 |
| SIG2 | 0.00695 | 0.06070 | 0.06191 | -0.03321 |
| SIG4 | 0.08368 | 0.07782 | -0.04808 | 0.02375 |

20 percent damped psv (cm/s)

| COEF | C0 | C1 | C2 | C3 |
|---|---|---|---|---|
| B1 | 1.40374 | 1.35854 | -1.88149 | 0.71782 |
| B2 | 0.31205 | -0.17374 | 0.60040 | -0.28394 |
| B3 | -0.08130 | -0.01435 | 0.22199 | -0.14682 |
| H | 5.66338 | 3.63138 | -15.22173 | 9.13430 |
| B5 | -0.89164 | -0.02480 | 0.08096 | -0.02094 |
| BV | -0.25076 | -0.06079 | -0.90611 | 0.56054 |
| LOGVA | 3.17909 | 0.79899 | -1.45838 | 0.67158 |
| SIG1 | 0.16865 | 0.00125 | 0.04311 | -0.01424 |
| SIG2 | 0.02248 | 0.00721 | 0.13665 | -0.07236 |
| SIG4 | 0.08637 | 0.06515 | -0.05932 | 0.03907 |

Table 9. Coefficients for larger component as a cubic function of log t for site effect in terms of continuous shear velocity.

2 percent damped psv (cm/s)

| COEF | C0 | C1 | C2 | C3 |
|------|------|------|------|------|
| B1 | 1.85796 | 2.10449 | -3.86361 | 1.78453 |
| B2 | 0.33735 | 0.02393 | 0.09652 | -0.01644 |
| B3 | -0.12183 | -0.10318 | 0.44112 | -0.23046 |
| H | 6.47604 | 13.98567 | -41.57274 | 23.87958 |
| B5 | -0.95121 | -0.23530 | 1.04519 | -0.63494 |
| BV | -0.18756 | 0.14232 | -1.50203 | 0.87573 |
| LOGVA | 2.97650 | 2.32001 | -3.96875 | 1.83679 |
| SIG1 | 0.20725 | -0.03834 | 0.08832 | -0.03828 |
| SIG2 | -0.00940 | 0.10622 | -0.04323 | 0.05615 |
| SIG4 | 0.00000 | 0.00000 | 0.00000 | 0.00000 |

5 percent damped psv (cm/s)

| COEF | C0 | C1 | C2 | C3 |
|------|------|------|------|------|
| B1 | 1.70003 | 1.97979 | -3.22270 | 1.40062 |
| B2 | 0.32059 | -0.02727 | 0.24853 | -0.09759 |
| B3 | -0.10401 | -0.15801 | 0.51107 | -0.26515 |
| H | 6.18210 | 10.61936 | -33.14299 | 19.21283 |
| B5 | -0.92151 | -0.22383 | 0.76539 | -0.44561 |
| BV | -0.20688 | 0.05736 | -1.16511 | 0.67327 |
| LOGVA | 3.03221 | 1.96183 | -3.37489 | 1.56641 |
| SIG1 | 0.19415 | -0.01519 | 0.07312 | -0.03526 |
| SIG2 | -0.01134 | 0.11701 | -0.05236 | 0.05945 |
| SIG4 | 0.00000 | 0.00000 | 0.00000 | 0.00000 |

10 percent damped psv (cm/s)

| COEF | C0 | C1 | C2 | C3 |
|------|------|------|------|------|
| B1 | 1.56253 | 1.71556 | -2.43821 | 0.97456 |
| B2 | 0.32384 | -0.06350 | 0.34072 | -0.15288 |
| B3 | -0.10648 | -0.10248 | 0.40387 | -0.21639 |
| H | 5.59958 | 7.90340 | -25.16582 | 14.63759 |
| B5 | -0.88607 | -0.20312 | 0.49729 | -0.26520 |
| BV | -0.21500 | -0.04212 | -0.87726 | 0.52041 |
| LOGVA | 3.08843 | 1.70863 | -2.99685 | 1.39965 |
| SIG1 | 0.18659 | -0.02435 | 0.09240 | -0.04125 |
| SIG2 | -0.00098 | 0.08911 | 0.00870 | 0.02598 |
| SIG4 | 0.00000 | 0.00000 | 0.00000 | 0.00000 |

20 percent damped psv (cm/s)

| COEF | C0 | C1 | C2 | C3 |
|------|------|------|------|------|
| B1 | 1.44367 | 1.41124 | -1.81388 | 0.69053 |
| B2 | 0.32379 | 0.04440 | 0.13760 | -0.05847 |
| B3 | -0.10169 | -0.06309 | 0.31892 | -0.17940 |
| H | 5.43053 | 4.06257 | -16.03367 | 9.71543 |
| B5 | -0.87365 | -0.15375 | 0.29499 | -0.14823 |
| BV | -0.23244 | -0.00352 | -0.87542 | 0.51529 |
| LOGVA | 3.18688 | 1.25622 | -2.28521 | 1.06378 |
| SIG1 | 0.17835 | -0.02316 | 0.08933 | -0.03507 |
| SIG2 | 0.00122 | 0.02929 | 0.13472 | -0.05018 |
| SIG4 | 0.00000 | 0.00000 | 0.00000 | 0.00000 |

Table 10.  Changes in Site Classification

| Sta_Code | Name | G(old) | G(new) |
|----------|------|--------|--------|
| 455 | Capitola | B | C |
| 498 | Halls Valley | B | C |
| 496 | SAGO South | A | B |
| 458 | San Francisco: Diamond Heights | A | B |

Table 11: Borehole Information (AvgVel in m/s).

| HOLE# | SITE NAME | LAT. | LONG. | AVGVEL | COMMENTS | REFERENCE |
|---|---|---|---|---|---|---|
| 209 | Monterey | 36.597 | 121.897 | 763 | extrpltd 10.49m to 30 m (based on El Granada, OFR 75-564). | Thiel and Schneider (1993) |
| 210 | Belmont | 37.512 | 122.308 | 628 | no tt extrapolation | Thiel and Schneider (1993) |
| 211 | Sago South (Hollister Hills) | 36.753 | 121.396 | 612 | extrapolated 10.49m to 30m (needs 6993 m/s to reach 750 m/s). | Thiel and Schneider (1993) |
| 212 | Piedmont Jr. High School | 37.823 | 122.233 | 896 | extrpltd 2m to 30m | Thiel and Schneider (1993) |
| 213 | San Francisco, Rincon Hill | 37.786 | 122.391 | 872 | extrpltd 5.9 m to 30 m. | Thiel and Schneider (1993) |
| 214 | San Francisco, Pacific Heights | 37.790 | 122.429 | 1250 | no tt extrapolation | Thiel and Schneider (1993) |
| 215 | Lexington Dam | 37.202 | 121.949 | 1071 | tt extrpltd 7.51m to 30m | Thiel and Schneider (1993) |
| 216 | San Francisco, Diamond Heights | 37.740 | 122.433 | 584 | extrapolated 0.1 m to 30 m. | Thiel and Schneider (1993) |
| 217 | Point Bonita | 37.820 | 122.520 | 1316 | tt extrapolation (but used suspension logging results) | Thiel and Schneider (1993) |
| 218 | Berkeley, Haviland Hall | 37.870 | 122.260 | 1266 | no tt extrapolation | Thiel and Schneider (1993) |
| 219 | Capitola | 36.974 | 121.952 | 289 | no tt extrapolation | Thiel and Schneider (1993) |
| 220 | So. San Francisco, Sierra Poin | 37.674 | 122.388 | 1020 | tt extrapolated 2.81 m to 30 m. | Thiel and Schneider (1993) |
| 221 | Agnews Hospital | 37.397 | 121.952 | 264 | no tt extrapolation | Thiel and Schneider (1993) |
| 222 | Livermore, Patterson Pass | 37.702 | 121.684 | 377 | tt extrapolated 0.1 m to 30 m. | Thiel and Schneider (1993) |
| 223 | Martinez V. A. Hospital | 37.993 | 122.115 | 384 | no tt extrapolation | Thiel and Schneider (1993) |
| 224 | Mission San Jose | 37.530 | 121.919 | 368 | no tt extrapolation | Thiel and Schneider (1993) |
| 225 | Santa Cruz | 37.001 | 122.060 | | no subsurface geophysics, shallow hole with voids | Thiel and Schneider (1993) |
| 226 | Richmond City | 37.935 | 122.342 | 260 | no tt extrapolation | Thiel and Schneider (1993) |
| 227 | Menlo Park V. A. Hospital | 37.468 | 122.157 | 267 | no tt extrapolation | Thiel and Schneider (1993) |
| 229 | San Francisco VA Medical Cente | 37.783 | 122.504 | 550 | no tt extrapolation | Thiel and Schneider (1993) |
| 230 | Halls Valley - Grant Park | 37.338 | 121.714 | 265 | no tt extrapolation | Thiel and Schneider (1993) |
| 231 | UC Berkeley Memorial Stadium | 37.870 | 122.250 | 472 | no tt extrapolation | Thiel and Schneider (1993) |
| 232 | Oakland Two Story | 37.806 | 122.267 | 323 | velocity based on suspension log; CUREE hole closer to sm than USG | Thiel and Schneider (1993) |
| 233 | Lawrence Livermore, Site 300 | | | 685 | coordinates not given in CUREE report; LLNL recorded LP89 here. | Thiel and Schneider (1993) |

Note: AVGVEL = 30m divided by the travel time to 30m; units are m/s.
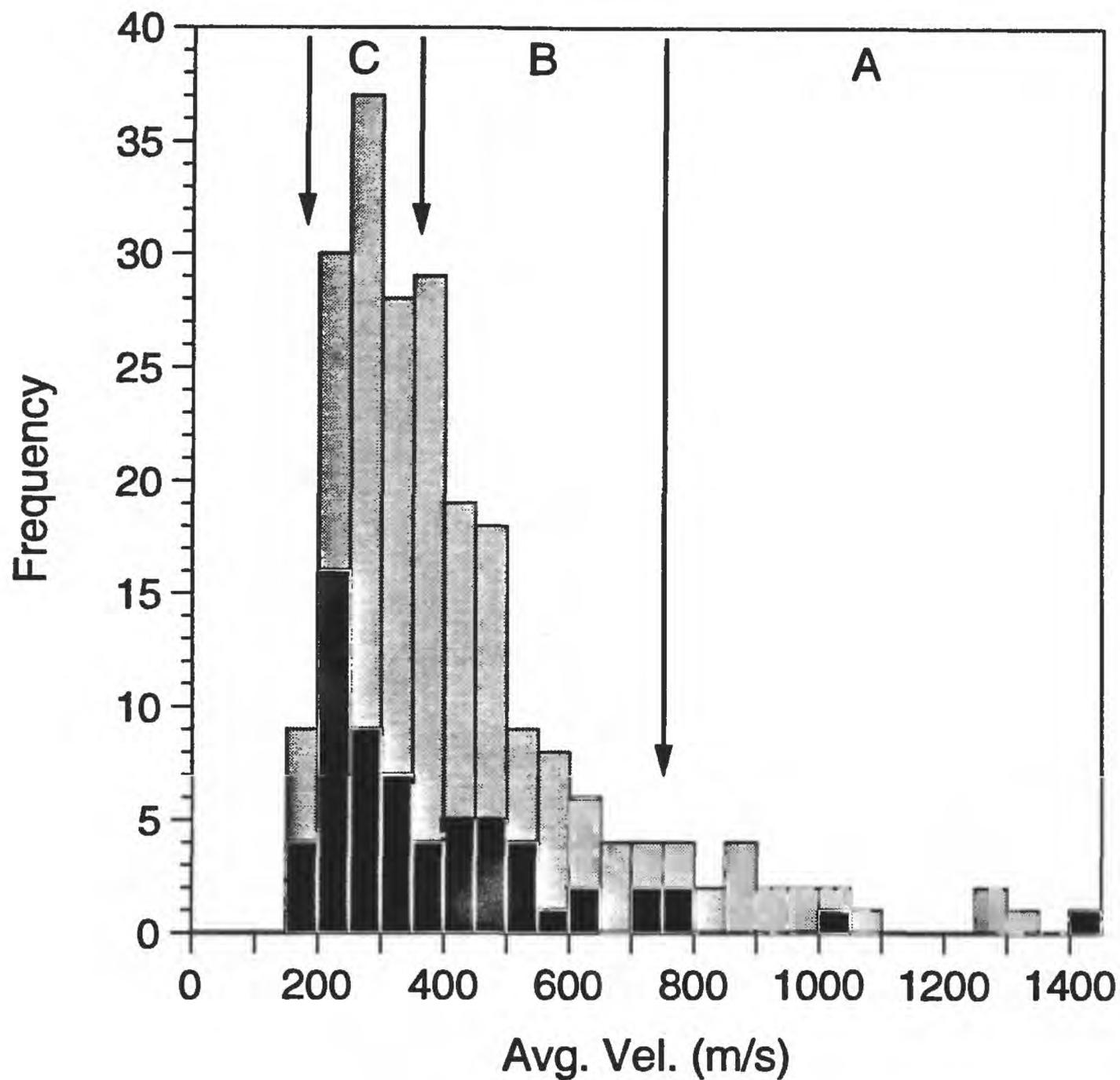
Figure 1. Histogram of average velocities, with boundaries between site classes shown by the arrows. The black bars are for those sites used in the regression analysis to determine the velocity dependence of response spectra, and the gray bars represent the distribution of the published shear-velocity data. It should be noted that the distribution shown by the gray bars does not necessarily represent the distribution that would be obtained for the shear-wave velocities from the population of strong-motion stations.
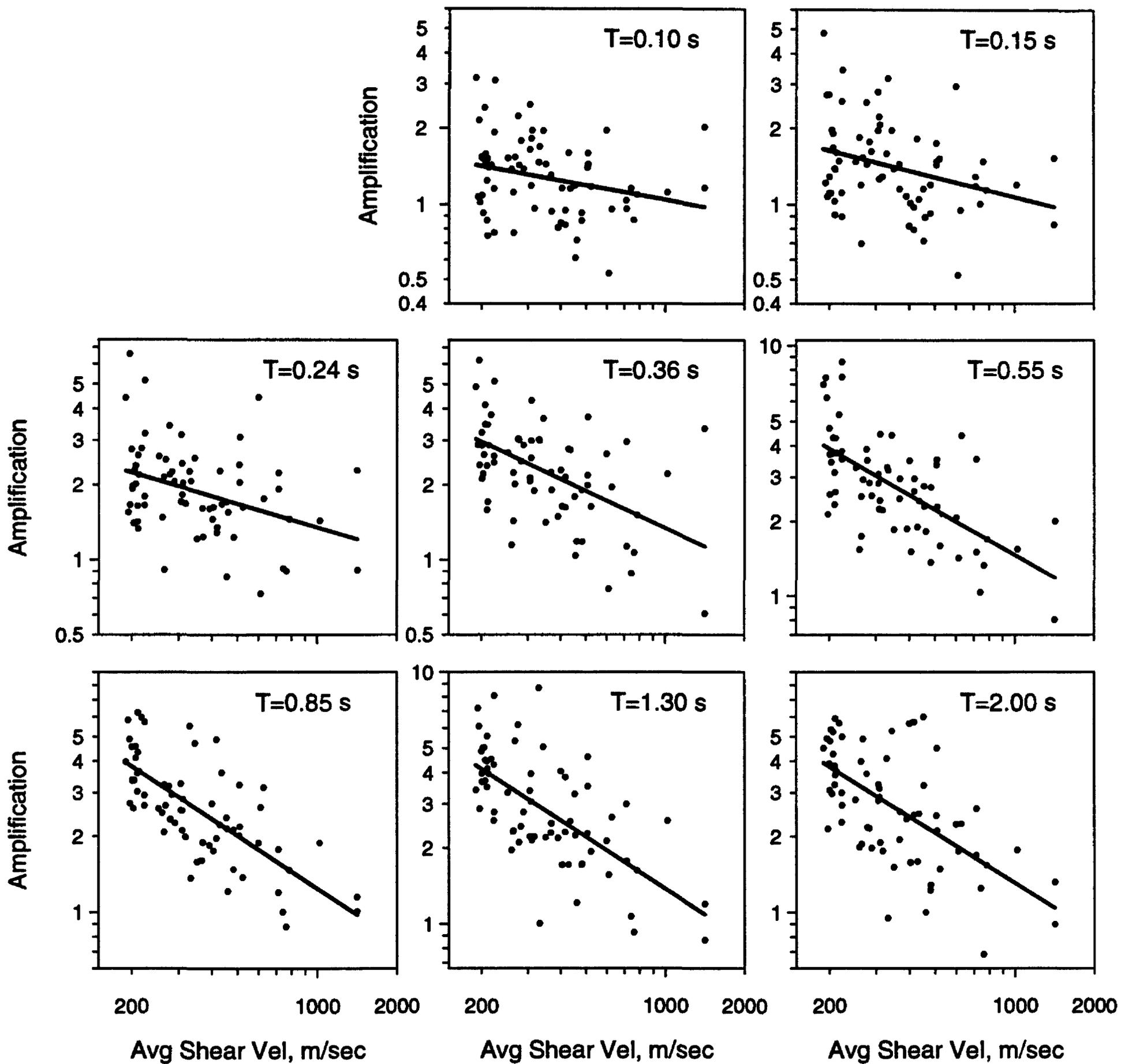
Figure 2. Amplification of 5 percent-damped response spectra for the random component as a function of average shear velocity, as given by equation (3). $T$ is the oscillator period, in seconds. The dots are the data used to determine the velocity dependence.
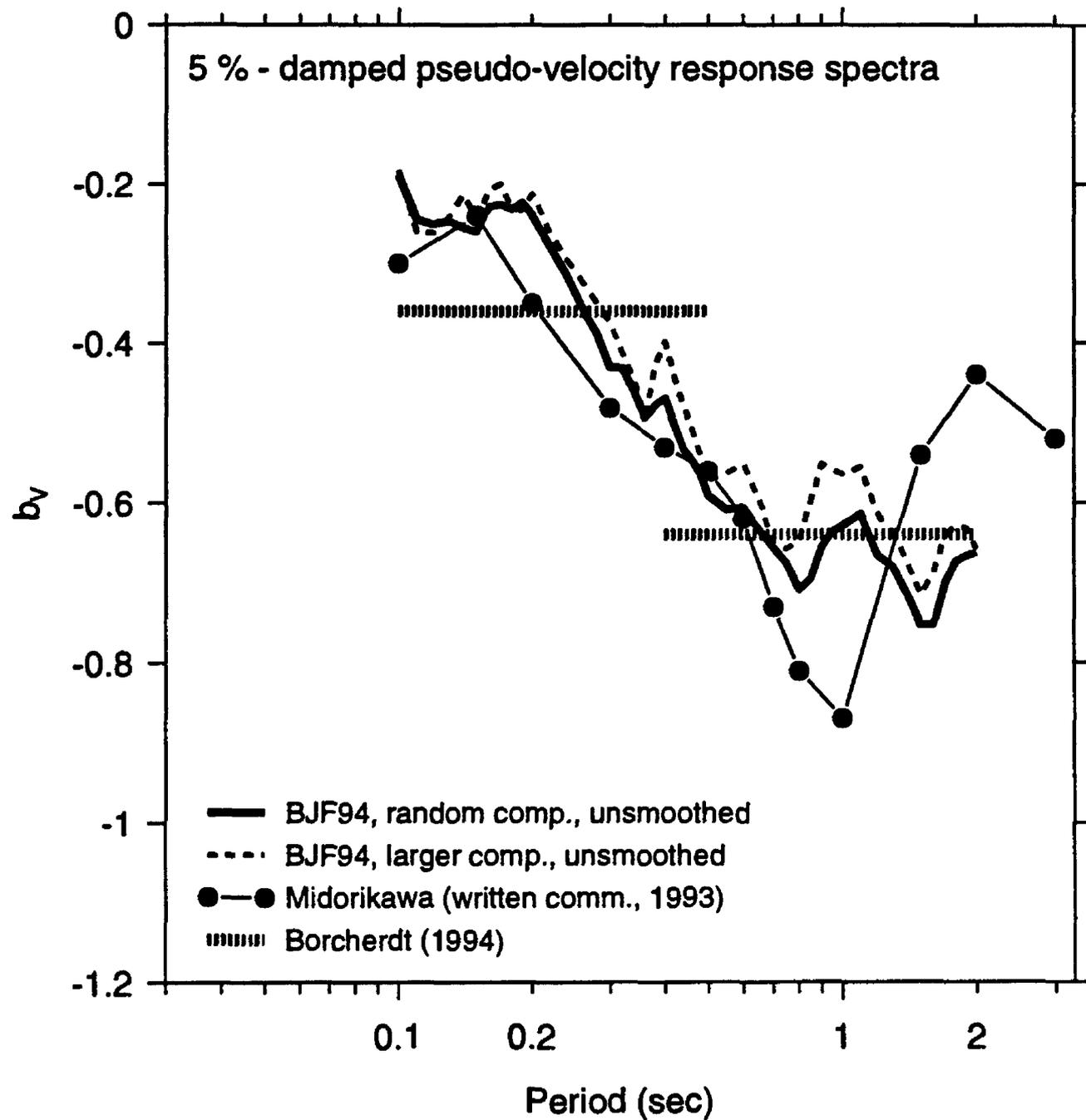
Figure 3. The coefficient that controls the shear-velocity dependence of response spectral amplification, as determined in this study for California data and by Midorikawa (written communication, 1993) for data from Japan. Also shown are the coefficients proposed by Borcherdt (1994) for determining short-period and mid-period amplification factors in building codes; these were determined from Fourier amplitude spectra of recordings from the Loma Prieta earthquake.
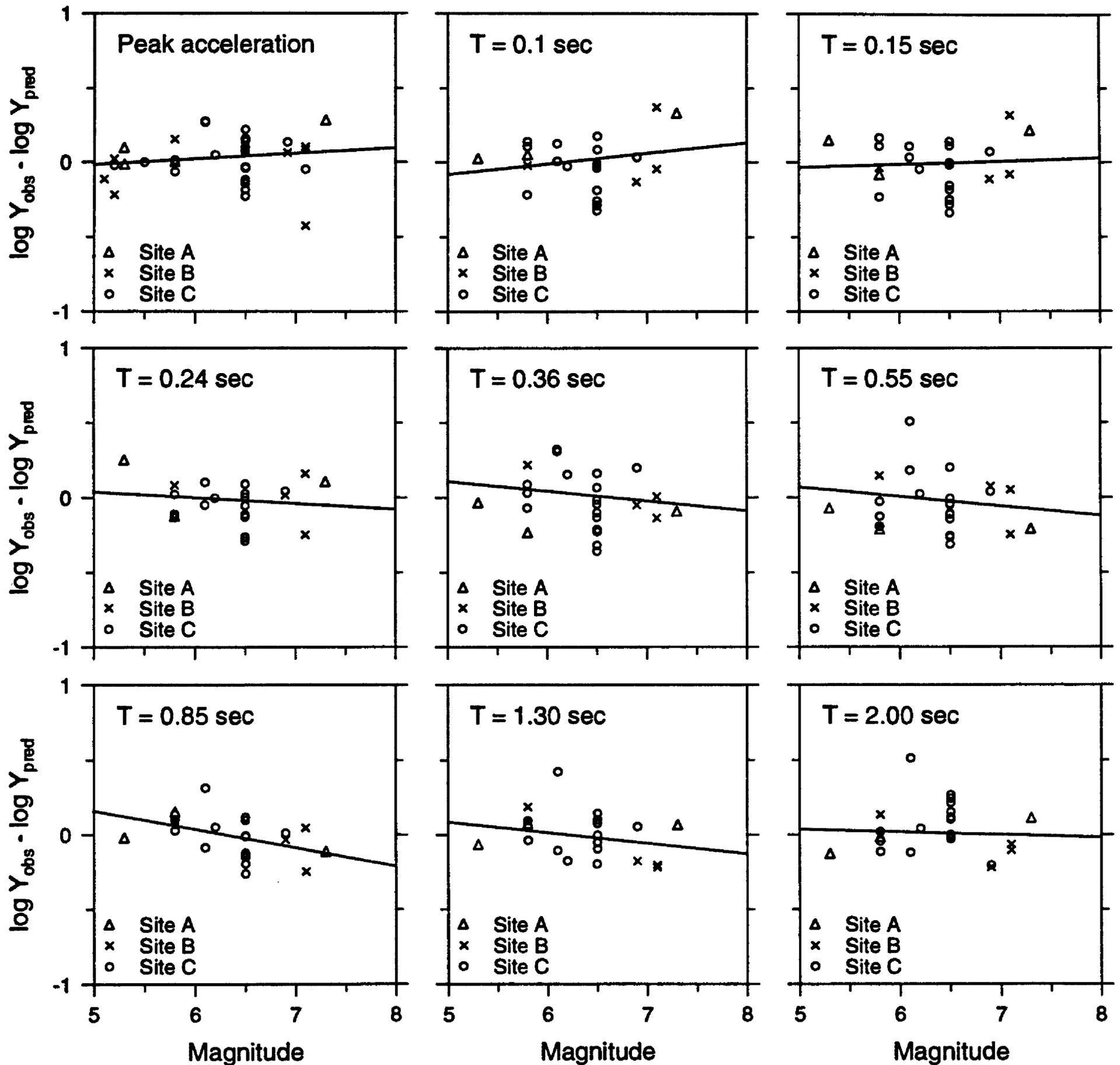
Figure 4. Residuals of peak acceleration and 5 percent-damped response spectra for the random component at distances less than 10 km, with straight line fit to the residuals. $T$ is the oscillator period, in seconds. The only slope that is significantly different than zero is that for the 0.85 sec oscillator.
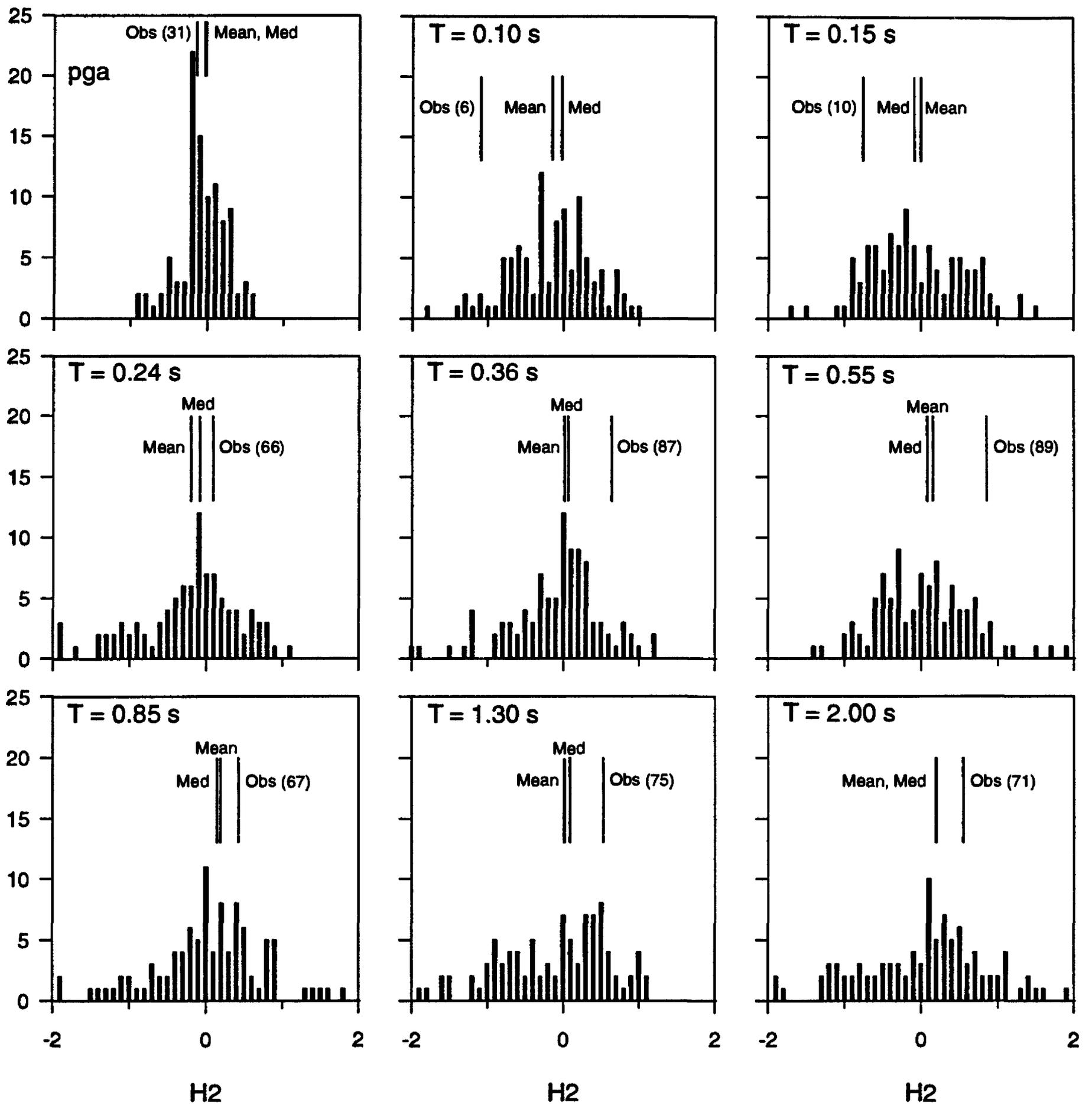
Figure 5. Histograms of $h_2$ determined from regression analyses of 100 simulated data sets obtained by setting $h_2 = 0$, for peak acceleration and 5 percent-damped response spectra, random component. $T$ is the oscillator period, in seconds. The lines show the mean and median values of $h_2$ from the simulated data, as well as the value of $h_2$ obtained from analysis of the observed data. The number in parenthesis after "Obs" is the percentage of $h_2$'s from the simulated data that fall below the value obtained from the observed data.
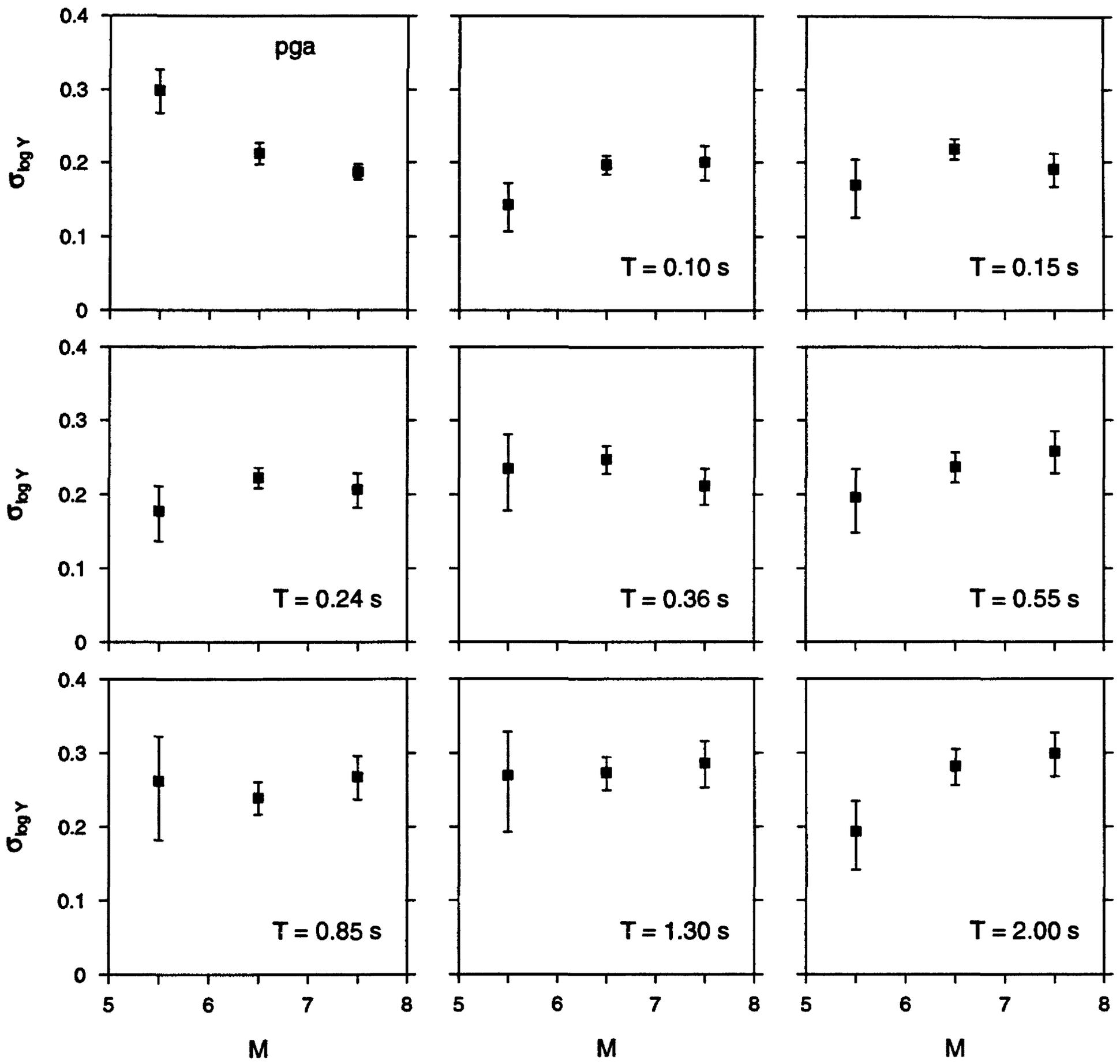
Figure 6. $\sigma_{\log Y}$ as a function of **M**, for peak acceleration and 5 percent-damped response spectra, random component. $T$ is the oscillator period, in seconds.

36
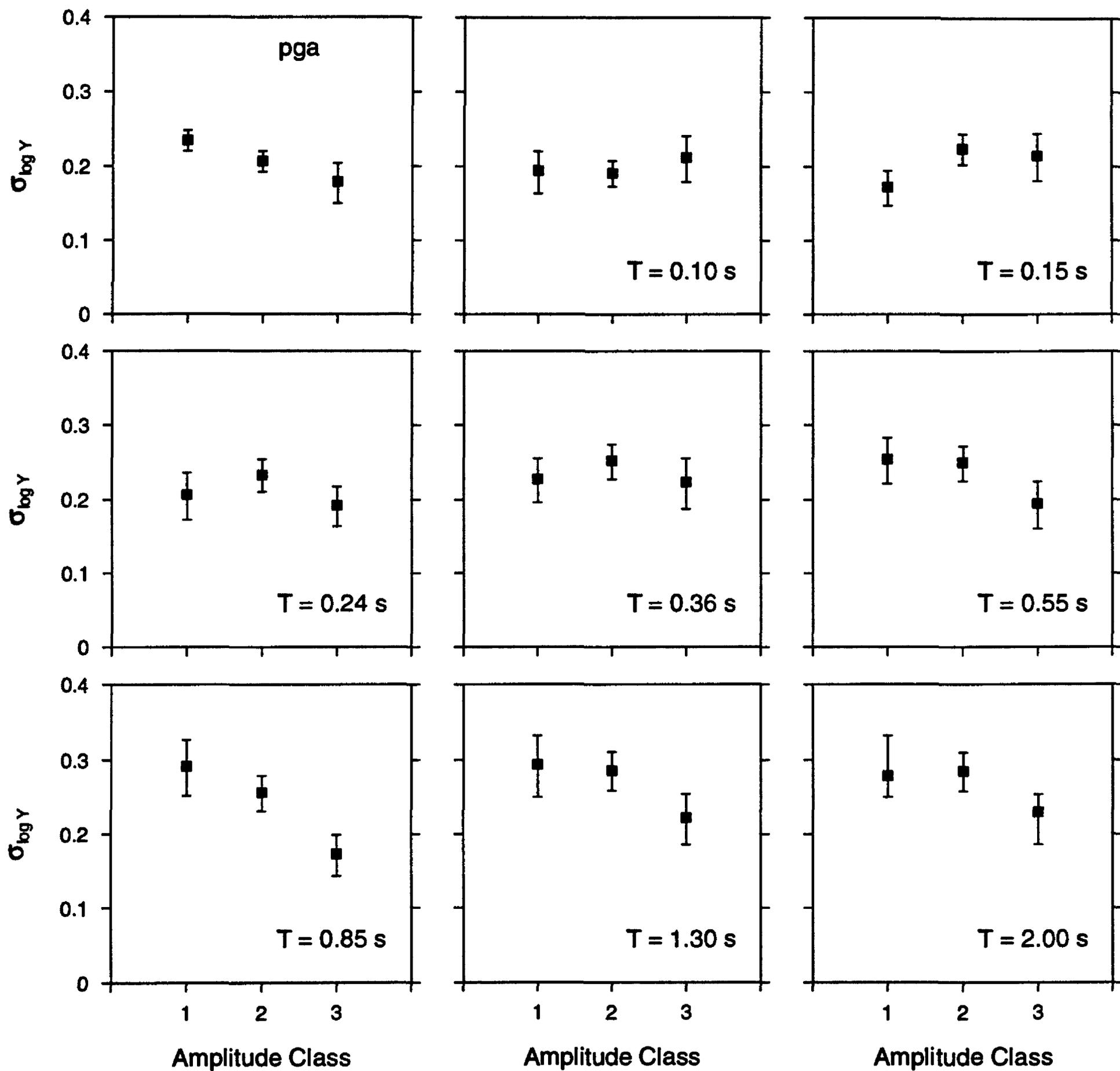
Figure 7. $\sigma_{\log Y}$ as a function of amplitude class, for peak acceleration and 5 percent-damped response spectra, random component. $T$ is the oscillator period, in seconds.
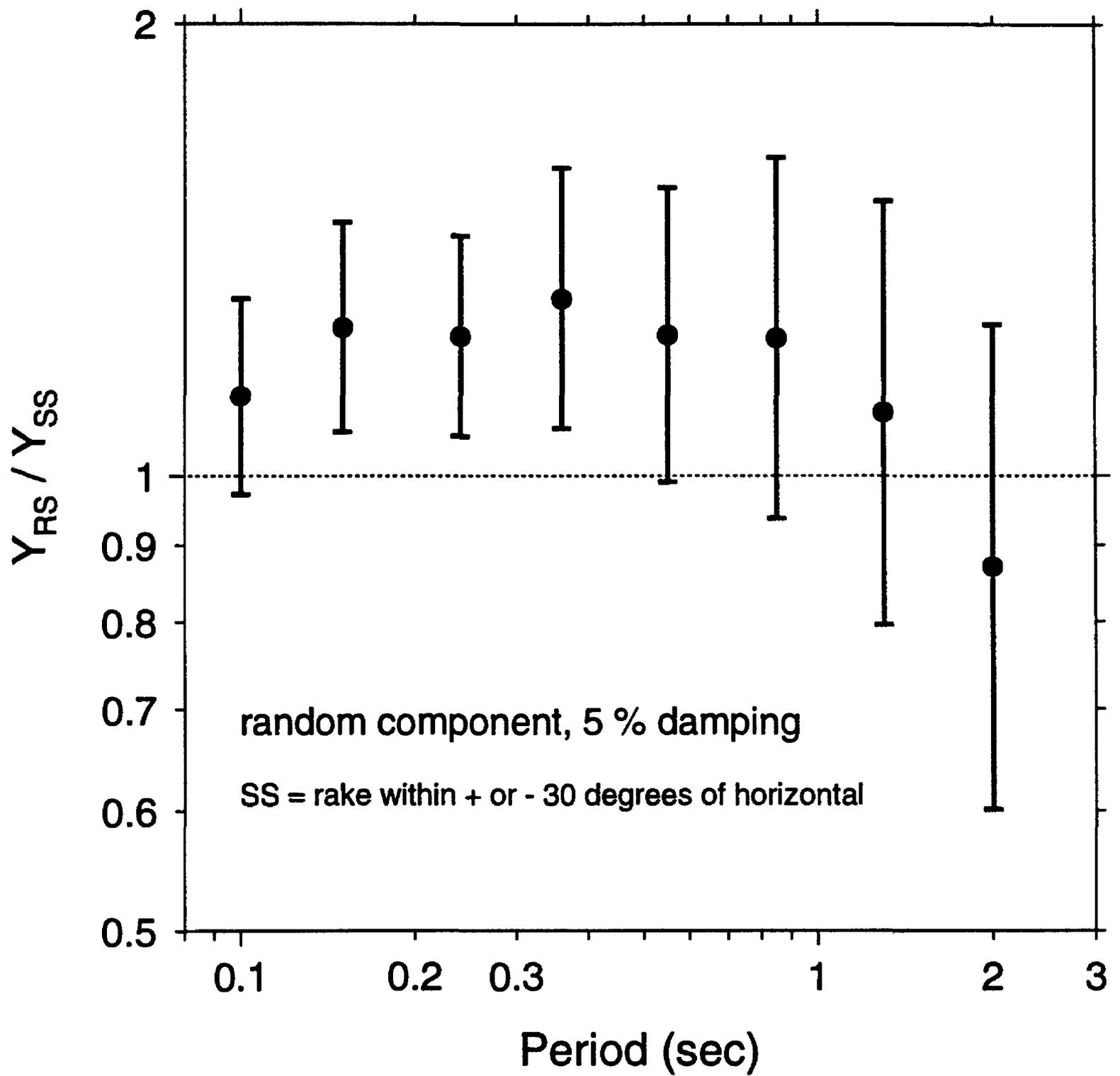
Figure 8. Ratio of response spectral values between reverse-slip and strike-slip earthquakes, as a function of oscillator period.
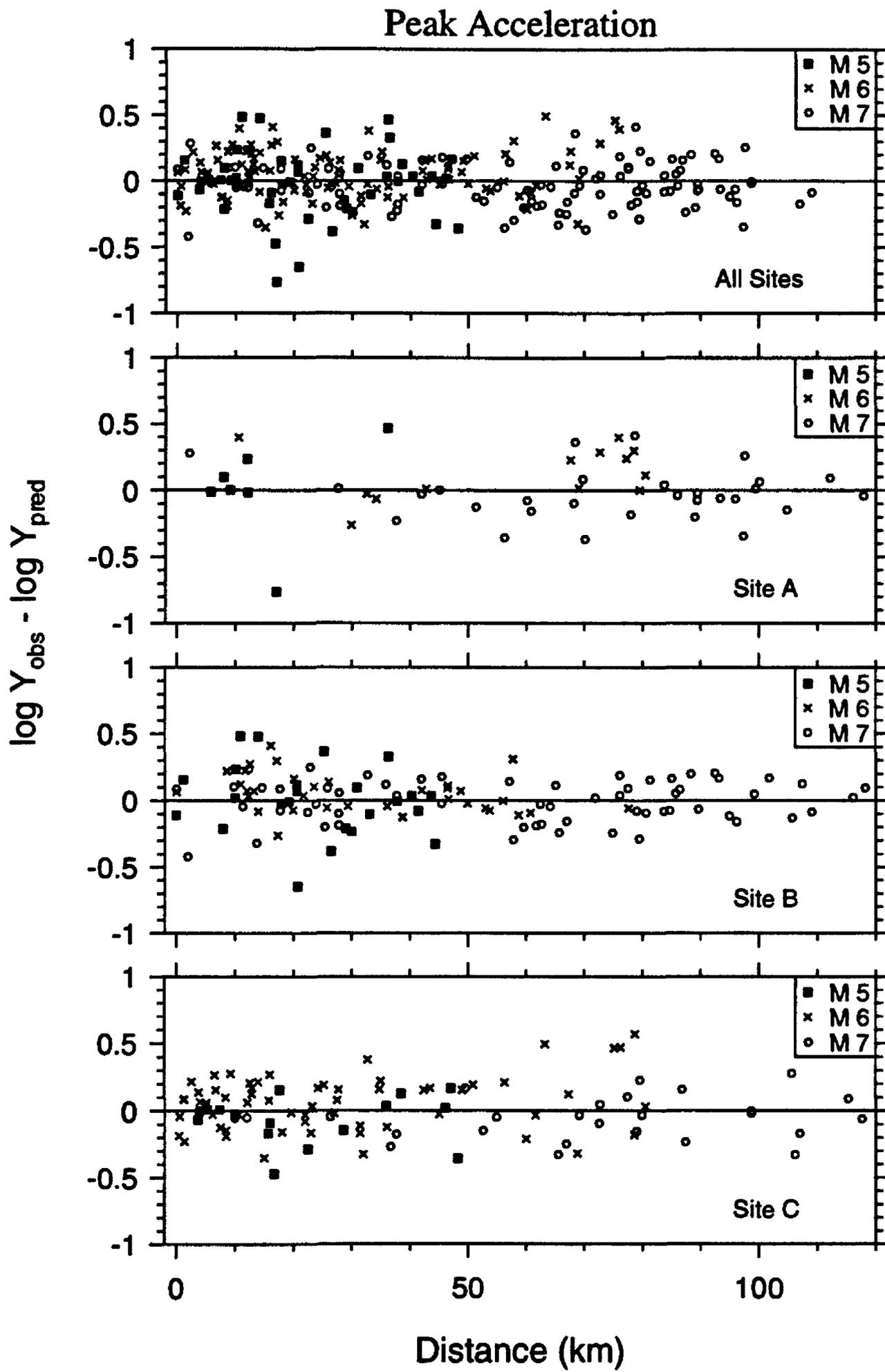
## Peak Acceleration



Figure 9. Residuals for peak acceleration.
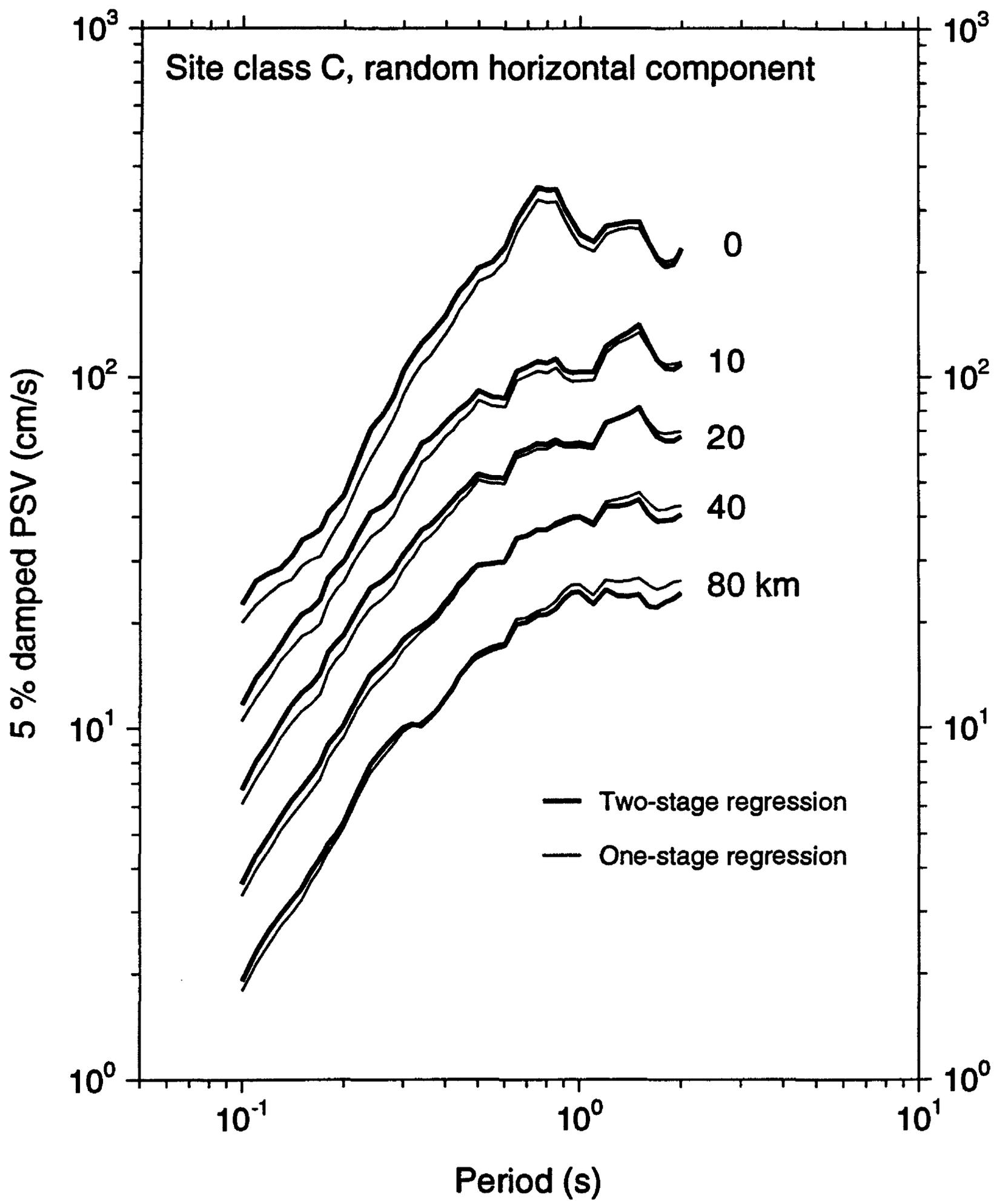
Figure 10. Comparison of one and two-stage regressions.